

Role of Phosphatidylserine in Phospholipid Flippase-Mediated Vesicle Transport in *Saccharomyces cerevisiae*

Miyoko Takeda, Kanako Yamagami, Kazuma Tanaka

Division of Molecular Interaction, Institute for Genetic Medicine, Hokkaido University, Graduate School of Life Science, Kita-ku, Sapporo, Japan

Phospholipid flippases translocate phospholipids from the exoplasmic to the cytoplasmic leaflet of cell membranes to generate and maintain phospholipid asymmetry. The genome of budding yeast encodes four heteromeric flippases (Drs2p, Dnf1p, Dnf2p, and Dnf3p), which associate with the Cdc50 family noncatalytic subunit, and one monomeric flippase Neo1p. Flippases have been implicated in the formation of transport vesicles, but the underlying mechanisms are largely unknown. We show here that overexpression of the phosphatidylserine synthase gene *CHO1* suppresses defects in the endocytic recycling pathway in flippase mutants. This suppression seems to be mediated by increased cellular phosphatidylserine. Two models can be envisioned for the suppression mechanism: (i) phosphatidylserine in the cytoplasmic leaflet recruits proteins for vesicle formation with its negative charge, and (ii) phosphatidylserine flipping to the cytoplasmic leaflet induces membrane curvature that supports vesicle formation. In a mutant depleted for flippases, a phosphatidylserine probe GFP-Lact-C2 was still localized to endosomal membranes, suggesting that the mere presence of phosphatidylserine in the cytoplasmic leaflet is not enough for vesicle formation. The *CHO1* overexpression did not suppress the growth defect in a mutant depleted or mutated for all flippases, suggesting that the suppression was dependent on flippase-mediated phospholipid flipping. Endocytic recycling was not blocked in a mutant lacking phosphatidylserine or depleted in phosphatidylethanolamine, suggesting that a specific phospholipid is not required for vesicle formation. These results suggest that flippase-dependent vesicle formation is mediated by phospholipid flipping, not by flipped phospholipids.

Type 4 P-type ATPases (P4-ATPases), highly conserved membrane proteins among eukaryotic cells, are phospholipid flippases that selectively transport phosphatidylserine (PS) and phosphatidylethanolamine (PE) from the exoplasmic to the cytoplasmic leaflet of the plasma membrane and internal membranes to generate and maintain asymmetrical distribution of phospholipids (1–4). P4-ATPase deficiencies are associated with human diseases (e.g., intrahepatic cholestasis type 1) (5). However, much remains to be learned about the functions and physiological and pathological importance of P4-ATPases.

In the budding yeast *Saccharomyces cerevisiae*, there are five P4-ATPases: Drs2p, Dnf1p, Dnf2p, Dnf3p, and Neo1p. Of these, Drs2p, Dnf1p/Dnf2p, and Dnf3p form complexes with the Cdc50 family noncatalytic subunits Cdc50p, Lem3p, and Crf1p, respectively, for their exit out of the endoplasmic reticulum (ER) and proper localization (6, 7). These four flippases are collectively essential for viability and have redundant roles for vesicle transport in various transport pathways (8, 9), including the early endosome-*trans*-Golgi network (TGN) retrieval pathway or the endocytic recycling pathway (7). Neo1p does not associate with Cdc50 family members and thus might function without a noncatalytic subunit. Neo1p is an essential protein by itself, possibly because it is involved in various cell functions other than the endocytic recycling pathway, including retrograde transport from Golgi bodies to the ER (10) and membrane trafficking within endosomal/Golgi system (11).

Amino phospholipids, PS and PE seem to be preferred substrates of flippases. *In vitro* studies using a fluorescent analog (NBD-PS and NBD-PE) suggested that Cdc50p-Drs2p prefers PS with a minor activity toward PE (12–14). In contrast, Lem3p-Dnf1p and -Dnf2p translocate NBD-PE and NBD-PC when they are localized at the plasma membrane (9, 15). However, since all of these studies essentially used a phospholipid analog or a lipid-

binding peptide, it needs to be further demonstrated that phospholipids are involved in flippase functions *in vivo*.

Cdc50p-Drs2p, which is mainly localized to early endosome/TGN membranes, is implicated in the formation of clathrin-coated vesicles from these membranes (16–19). Because clathrin has no intrinsic lipid-binding ability, it is linked to membranes by adaptors, which bind to lipids and/or the cytoplasmic domains of cargo proteins (20). The AP-1 clathrin adaptor has been suggested to function downstream of Cdc50p-Drs2p (18, 19), but the underlying mechanisms are unknown.

One important question is how flippase activity is harnessed to form a transport vesicle. Flippases would influence physicochemical properties of membranes by an asymmetric membrane structure with a high concentration of substrate lipids, such as PS and PE, in the cytoplasmic leaflet. These phospholipids could recruit adaptor proteins for vesicle formation by their specific properties (e.g., a negative charge of PS). A second important consequence of a flippase activity is an increase in phospholipid number within the cytoplasmic leaflet relative to the luminal leaflet. This could induce bending in the membrane toward the cytosol, a process that is essential to vesicle budding (21).

We show here that overexpression of the PS synthase gene *CHO1*, which resulted in an increase in PS, suppressed defects in the endocytic recycling of flippase mutants. Our results suggest that PS in the cytoplasmic leaflet is not sufficient for vesicle for-

Received 17 October 2013 Accepted 26 December 2013

Published ahead of print 3 January 2014

Address correspondence to Kazuma Tanaka, k-tanaka@igm.hokudai.ac.jp.

Copyright © 2014, American Society for Microbiology. All Rights Reserved.

doi:10.1128/EC.00279-13

TABLE 1 Yeast strains used in this study

Strain ^a	Relevant genotype	Source or reference
YEF473	<i>MATa</i> α <i>lys2-801/lys2-801 ura3-52/ira3-52 his3Δ-200/his3Δ-200 trp1Δ-63/trp1Δ-63 leu2Δ-1/leu2Δ-1</i>	26
YKT1066	<i>MATa</i> <i>lys2-801 ura3-52 his3Δ-200 leu2Δ-1 TRP1</i>	This study
YKT1651	<i>MATa</i> <i>neo1-101</i>	This study
YKT1781	<i>MATa</i> <i>neo1-101::LEU2 TRP1</i>	This study
YKT1782	<i>MATa</i> <i>KanMX6::P_{GAL1}-3HA-CDC50 TRP1</i>	This study
YKT1783	<i>MATa</i> <i>HphMX4::P_{GAL1}-3HA-CDC50 neo1-101::LEU2 TRP1</i>	This study
YKT1629	<i>MATa</i> <i>TRP1::P_{GAL1}-DRS2</i>	This study
YKT1784	<i>MATa</i> <i>TRP1::PGAL1-DRS2 neo1-101</i>	This study
YKT1785	<i>MATa</i> <i>DNF2-EGFP::natMX TRP1</i>	This study
YKT1786	<i>MATa</i> <i>neo1-101::LEU2 DNF2-EGFP::natMX TRP1</i>	This study
YKT1787	<i>MATa</i> <i>KanMX6::P_{GAL1}-3HA-CDC50 DNF2-EGFP::KanMX6 TRP1</i>	This study
YKT1788	<i>MATa</i> <i>HphMX4::P_{GAL1}-3HA-CDC50 neo1-101::LEU2 DNF2-EGFP::natMX TRP1</i>	This study
YKT1777	<i>MATa</i> <i>LEU2::mRFP-SNC1 TRP1</i>	This study
YKT1789	<i>MATa</i> <i>HphMX4::P_{GAL1}-3HA-CDC50 neo1-101::LEU2 LEU2::mRFP-SNC1 TRP1</i>	This study
YKT1790	<i>MATa</i> <i>HphMX4::P_{GAL1}-3HA-CDC50 neo1-101::LEU2 SEC7-mRFP::KanMX6 TRP1</i>	This study
YKT1650	<i>MATa</i> <i>HIS3MX6::P_{GAL1}-3HA-CDC50 neo1-101</i>	This study
YKT1529	<i>MATa</i> <i>KanMX6::P_{GAL1}-3HA-CDC50 dnf1Δ::HIS3MX6 crf1Δ::HphMX3 TRP1</i>	This study
YKT1791	<i>MATa</i> <i>KanMX6::P_{GAL1}-3HA-CDC50 dnf1Δ::HIS3MX6 crf1Δ::HphMX3 DNF2-EGFP::KanMX6 TRP1</i>	This study
YKT1792	<i>MATa</i> <i>KanMX6::P_{GAL1}-3HA-CDC50 dnf1Δ::HIS3MX6 crf1Δ::HphMX3 LEU2::GFP-SNC1 TRP1</i>	This study
YKT1793	<i>MATa</i> <i>TRP1::P_{GAL1}-3HA-CDC50 dnf1Δ::HIS3MX6 crf1Δ::HphMX3 LEU2::GFP-SNC1(p_m)</i>	This study
YKT1513	<i>MATa</i> <i>KanMX6::P_{GAL1}-3HA-CDC50 lem3Δ::HIS3MX6 crf1Δ::HphMX3 TRP1</i>	This study
YKT1660	<i>MATa</i> <i>KanMX6::P_{GAL1}-3HA-NEO1</i>	This study
YKT1796	<i>MATa</i> <i>HphMX4::P_{GAL1}-3HA-CDC50 neo1-101::LEU2 lem3Δ::HIS3MX6 crf1Δ::HphMX4 TRP1</i>	This study
YKT1797	<i>MATa</i> <i>DNF1-EGFP::KanMX6 TRP1</i>	67
YKT1798	<i>MATa</i> <i>HphMX4::P_{GAL1}-3HA-CDC50 neo1-101::LEU2 DNF1-EGFP::KanMX6 TRP1</i>	This study
YKT1799	<i>MATa</i> <i>LEU2::GFP-Lact-C2 TRP1</i>	This study
YKT1800	<i>MATa</i> <i>KanMX6::P_{GAL1}-3HA-CDC50 dnf1Δ::HIS3MX6 crf1Δ::HphMX3 LEU2::GFP-Lact-C2 TRP1</i>	This study
YKT1801	<i>MATa</i> <i>KanMX6::P_{GAL1}-3HA-CDC50 dnf1Δ::HIS3MX6 crf1Δ::HphMX3 LEU2::mRFP-SNC1 URA3::GFP-Lact-C2-AAA TRP1</i>	This study
YKT1802	<i>MATa</i> <i>KanMX6::P_{GAL1}-3HA-CDC50 KanMX6::P_{GAL1}-3HA-NEO1 lem3Δ::HIS3MX6 crf1Δ::HphMX3 URA3::GFP-Lact-C2 TRP1</i>	This study
YKT1428	<i>MATa</i> <i>cho1Δ::KanMX4 TRP1</i>	This study
YKT1642	<i>MATa</i> <i>APL2-EGFP::KanMX6 TRP1</i>	This study
YKT1803	<i>MATa</i> <i>cho1Δ::natMX APL2-EGFP::KanMX6 TRP1</i>	This study
YKT1507	<i>MATa</i> <i>cdc50Δ::HIS3MX6 TRP1</i>	This study
YKT1804	<i>MATa</i> <i>cdc50Δ::HphMX4 cho1Δ::KanMX4 TRP1</i>	This study
YKT1805	<i>MATa</i> <i>DNF2-EGFP::HphMX4 TRP1</i>	This study

TABLE 1 (Continued)

Strain ^a	Relevant genotype	Source or reference
YKT1806	<i>MATa</i> <i>cho1Δ::natMX DNF2-EGFP::KanMX6 TRP1</i>	This study
YKT1807	<i>MATa</i> <i>KanMX6::P_{GAL1}-3HA-CDC50 cho1Δ::natMX DNF2-EGFP::KanMX6 TRP1</i>	This study
YKT1808	<i>MATa</i> <i>KanMX6::P_{GAL1}-3HA-CDC50 cho1Δ::natMX SEC7-mRFP::KanMX6 DNF2-GFP::HphMX4 TRP1</i>	This study
YKT1809	<i>MATa</i> <i>psd1Δ::KanMX6 psd2Δ::HIS3MX6 TRP1</i>	This study
YKT1523	<i>MATa</i> <i>URA3::GFP-SNC1 TRP1</i>	64
YKT1810	<i>MATa</i> <i>psd1Δ::KanMX6 psd2Δ::HIS3MX6 URA3::GFP-SNC1 TRP1</i>	This study
YKT1871	<i>MATa</i> <i>SEC63-mRFP::KanMX6 TRP1</i>	This study
YKT1872	<i>MATa</i> <i>HphMX4::P_{GAL1}-3HA-CDC50 neo1-101::LEU2 SEC63-mRFP::KanMX6 TRP1</i>	This study

^a YKT strains are isogenic derivatives of YEF473.

mation and that flippase-mediated phospholipid translocation is coupled with vesicle formation.

MATERIALS AND METHODS

Media and genetic methods. Unless otherwise specified, strains were grown in YPDA rich medium (1% Bacto yeast extract [Difco Laboratories, Detroit, MI], 2% Bacto peptone [Difco], 2% glucose, and 0.01% adenine). Strains carrying plasmids were selected in synthetic medium (SD) containing the required nutritional supplements (22). Synthetic complete medium (SC) was SD medium containing all required nutritional supplements. When appropriate, 0.5% Casamino Acids were added to SD medium without uracil (SDA-U). For induction of the *GAL1* promoter, 3% galactose, and 0.2% sucrose were used as carbon sources instead of glucose (YPGA, SG-U, and SGA-U). When required, 2 mM ethanolamine and 2 mM choline were supplemented to medium to support growth of the *cho1 Δ* and *psd1 Δ psd2 Δ* mutants, respectively. Standard genetic manipulations of yeast were performed as described previously (23). The lithium acetate method was used for introduction of plasmids into yeast cells (24, 25). *Escherichia coli* strains DH5 α and XL1-Blue were used for construction and amplification of plasmids.

Strains and plasmids. Yeast strains constructed in the YEF473 background (26) are listed in Table 1. Because flippase and *cho1 Δ* mutants exhibit defects in tryptophan uptake (27), a strain in which *trp1 Δ -63* was replaced with *TRP1* was constructed (YKT1066), and most strains used in the present study were derived from this strain. PCR-based procedures were used to construct gene deletions and gene fusions with the *GAL1* promoter, green fluorescent protein (GFP), and mRFP (26). Some gene deletions (*psd1 Δ* and *psd2 Δ*) were constructed by transformation with PCR-products from knockout strains. The *psd1 Δ psd2 Δ* mutant was kindly provided by S. Moye-Rowley. All constructs produced by the PCR-based procedure were verified by colony-PCR amplification to confirm the replacement occurred at the expected locus. When required, selection markers of mutant alleles were changed appropriately by cassette exchange (28).

The GFP-tagged Lact-C2 plasmid (pRS416-GFP-Lact-C2) (29) was purchased from Hematologic Technologies, Inc. (Essex Junction, VT). The *URA3::GFP-Lact-C2* strain was constructed by integrating the linearized pRS306-GFP-Lact-C2 into the *URA3* locus, and the *URA3::GFP-Lact-C2AAA* (Lact-C2-W26A, W33A, F34A) strain was similarly constructed. *Lact-C2AAA* (29), *CHO1(D148A)*, and *CHO1(D152A)* mutations were constructed by site-directed mutagenesis as described previously (30). The *LEU2::mRFP-SNC1* strain was constructed by integrating the linearized pRS305-mRFP-SNC1 into the *LEU2* locus, and the *LEU2::mRFP-SNC1(p_m)* strain was similarly constructed. The *neo1-101::LEU2*

TABLE 2 Plasmids used in this study

Plasmid ^a	Characteristics	Source or reference
YE24	URA3 2 μ m	32
pRS425	LEU2 2 μ m	68
YEplac112	TRP1 2 μ m	69
YEplac181	LEU2 2 μ m	69
YEplac195	URA3 2 μ m	69
pKT1488 [pRS416-GFP-TLG1]	<i>P_{TRP1}-GFP-TLG1 URA3 CEN</i>	This study
pKT1443 [pRS416-GFP-SNC1]	<i>P_{TRP1}-GFP-SNC1 URA3 CEN</i>	38
pKT1753 [YE24-CHO1]	<i>CHO1 URA3 2μm</i>	This study
pKT1263 [YEplac195-CDC50]	<i>CDC50 URA3 2μm</i>	This study
pKT1964 [pRS416-mRFP-SNC1(pm)]	<i>P_{TRP1}-mRFP-SNC1(pm) URA3 CEN</i>	This study
pKT1788 [pRS425-NEO1]	<i>NEO1 LEU2 2μm</i>	This study
pKT2097 [YEplac112-CHO1]	<i>CHO1 TRP1 2μm</i>	This study
PKT2098 [YEplac112-LEM3]	<i>LEM3 TRP1 2μm</i>	This study
pKT1607 [YEplac195-DRS2-CDC50]	<i>DRS2-CDC50 URA3 2μm</i>	6
pKT1469 [YEplac195-NEO1]	<i>NEO1 URA3 2μm</i>	This study
pKT1602 [YEplac195-DNF1]	<i>DNF1 URA3 2μm</i>	67
pKT1340 [YEplac181-LEM3]	<i>LEM3 LEU2 2μm</i>	67
pKT1264 [YCplac22-CDC50]	<i>CDC50 TRP1 CEN</i>	This study
pKT1563 [pRS416-mRFP-SNC1]	<i>P_{TRP1}-mRFP-SNC1 URA3 CEN</i>	61
pKT1568 [pRS315-mRFP-SNC1]	<i>P_{TRP1}-mRFP-SNC1 LEU2 CEN</i>	This study
pKT1444 [pRS416-GFP-SNC1(pm)]	<i>P_{TRP1}-GFP-SNC1(pm) URA3 CEN</i>	38
pKT2096 [YE352-PSD2]	<i>PSD2 URA3 2μm</i>	53
pKT2099 [pRS305-mRFP-SNC1]	<i>P_{TRP1}-mRFP-SNC1 LEU2</i>	This study
pKT1749 [pRS416-GFP-Lact-C2]	<i>GFP-Lact-C2 URA3 CEN</i>	29
pKT2100 [pRS306-GFP-Lact-C2]	<i>GFP-Lact-C2 URA3</i>	This study
pKT1995 [pRS306-GFP-Lact-C2-AAA]	<i>GFP-Lact-C2-AAA URA3</i>	This study
pKT1807 [pRS316-NEO1]	<i>NEO1 URA3 CEN</i>	This study
pKT2102 [pRS305-neo1-101-C]	<i>neo1-101-C LEU2</i>	This study
pKT2101 [pRS305-GFP-Snc1(pm)]	<i>P_{TRP1}-GFP-SNC1(pm) LEU2</i>	This study
pKT2102 [pRS316-NEO1 Δ BglIII]	<i>NEO1ΔBglIII URA3 CEN</i>	This study
pKT2111 [YEplac195-CHO1]	<i>CHO1 URA3</i>	This study
pKT2112 [YEplac195-CHO1-GFP]	<i>CHO1-GFP URA3</i>	This study
pKT2114 [YEplac195-CHO1(D148A)]	<i>cho1(D148A) URA3</i>	This study
pKT2115 [YEplac195-CHO1(D152A)]	<i>cho1(D152A) URA3</i>	This study

^a Vector and gene names are indicated in brackets, where applicable.

strain was constructed by integrating the linearized pRS305-neo1-101-C, which contained only the carboxyl-terminal *neo1-101* mutation site fragment, into the *NEO1* locus. The plasmids used in the present study are listed in Table 2. Schemes detailing the construction of plasmids and DNA sequences of nucleotide primers are available upon request.

Determination of the *neo1-101* mutation site. The *neo1-101* mutant gene was cloned by the gap repair method (31). The pRS316-NEO1 Δ BglIII plasmid was linearized with HindIII and HpaI, followed by transformation into the *neo1-101* strain (YKT1651). Plasmids were recovered from several independent Ura⁺ transformants and sequenced. One mutation,

which changed GTG (Val) of the codon 1145 to ATG (Met) in the C-terminal cytosolic region of Neo1p, was identified.

Isolation of multicopy suppressors of the *P_{GALI}-CDC50 neo1-101* mutant. The *P_{GALI}-CDC50 neo1-101* strain was transformed with a yeast genomic DNA library constructed in the multicopy plasmid YE24 (32). Transformants were selected on SGA-U plate at 30°C and then replica plated onto YPDA plates. Plasmids were recovered from the transformants that grew on YPDA, and those containing *CDC50* or *NEO1* were identified by PCR and eliminated. Restriction enzyme digestion of the remaining plasmids indicated that 20 different clones were isolated. Nine of these plasmids reproducibly conferred growth on YPDA. Three clones that exhibited clearer suppression were chosen, and the genes responsible for the suppression were determined to be *CHO1*, *YCK1*, and *ART5* by fragment subcloning and DNA sequencing.

Microscopic observations. Cells were observed using a Nikon Eclipse E800 microscope (Nikon Instec, Tokyo, Japan) equipped with an HB-10103AF super high-pressure mercury lamp and a 1.4 numerical aperture 100 \times Plan Apo oil immersion objective lens with appropriate fluorescence filter sets or differential interference contrast optics. Images were acquired using a digital cooled charge-coupled device camera (C4742-95-12NR; Hamamatsu Photonics, Hamamatsu, Japan) using AQUACOSMOS software (Hamamatsu Photonics). Observations are compiled from the examination of at least 100 cells. To visualize GFP- or mRFP-tagged proteins, cells were grown to early to mid-logarithmic phase, harvested, and resuspended in SDA- or SD-based medium. Cells were mounted on microslide glass and immediately observed using a GFP band-pass or G-2A (for mRFP) filter set.

Phospholipid analysis. Cells were grown in 12 ml of appropriate medium containing 1 μ Ci of [³²P]orthophosphoric acid (Perkin-Elmer-Cetus, Norwalk)/ml to an optical density at 600 nm of 0.5 for 12 h at 30°C to achieve steady-state labeling. The cells were harvested by centrifugation, washed with sterile water, and transferred to screw-cap glass tubes. The cells were treated with 5% trichloroacetic acid for 1 h on ice and then washed with cold water three times. Phospholipids were extracted basically by the Bligh and Dyer method (33), using 0.1N HCl as the aqueous phase as described previously (34). The cells were resuspended in 1.2 ml of CHCl₃-methanol (MeOH)-0.1 N HCl (1:2:0.8) and lysed by vortexing with glass beads for 3 min. Then, 0.4 ml each of CHCl₃ and HCl/NaCl (0.1 N/0.5 M) was added, followed by centrifugation, isolation of the lipid-containing phase, and evaporation of the solvent. The extracted lipids were dissolved in appropriate volume of CHCl₃-MeOH (2:1) and analyzed by one-dimensional high-performance thin-layer chromatography (HPTLC) as described previously (35). The HPTLC plate (Merck, Darmstadt, Germany) was exposed to an imaging plate for 2 days, and the signal was detected and quantitated by using an FLA 3000 fluorescent image analyzer (Fuji Film, Tokyo, Japan). Phospholipids were identified by comparison to commercial standards (Avanti Polar Lipids, Alabaster, AL).

RESULTS

Combination of *neo1-101* and *cdc50 Δ* mutations results in synthetic defects in endocytic recycling. We previously screened for mutations that were synthetically lethal with *cdc50 Δ* and obtained an allele of *NEO1*, *neo1-101* (36). Neo1-101p had a valine 1145-to-methionine substitution in the C-terminal cytoplasmic region. *NEO1* is an essential gene, but the *neo1-101* mutation did not affect the growth rate (Fig. 1A). The *neo1-101* mutation was combined with conditional alleles of flippase genes, *P_{GALI}-CDC50* and *P_{GALI}-DRS2* alleles, whose expression is repressed by glucose. Both Cdc50p- and Drs2p-depleted *neo1-101* cells exhibited severe growth defects (Fig. 1A). The *neo1-101* mutation did not exhibit synthetic growth defects with *lem3 Δ* or *dnf1 Δ dnf2 Δ* mutations (data not shown).

Because a previous study showed that Cdc50p-Drs2p, Lem3p-

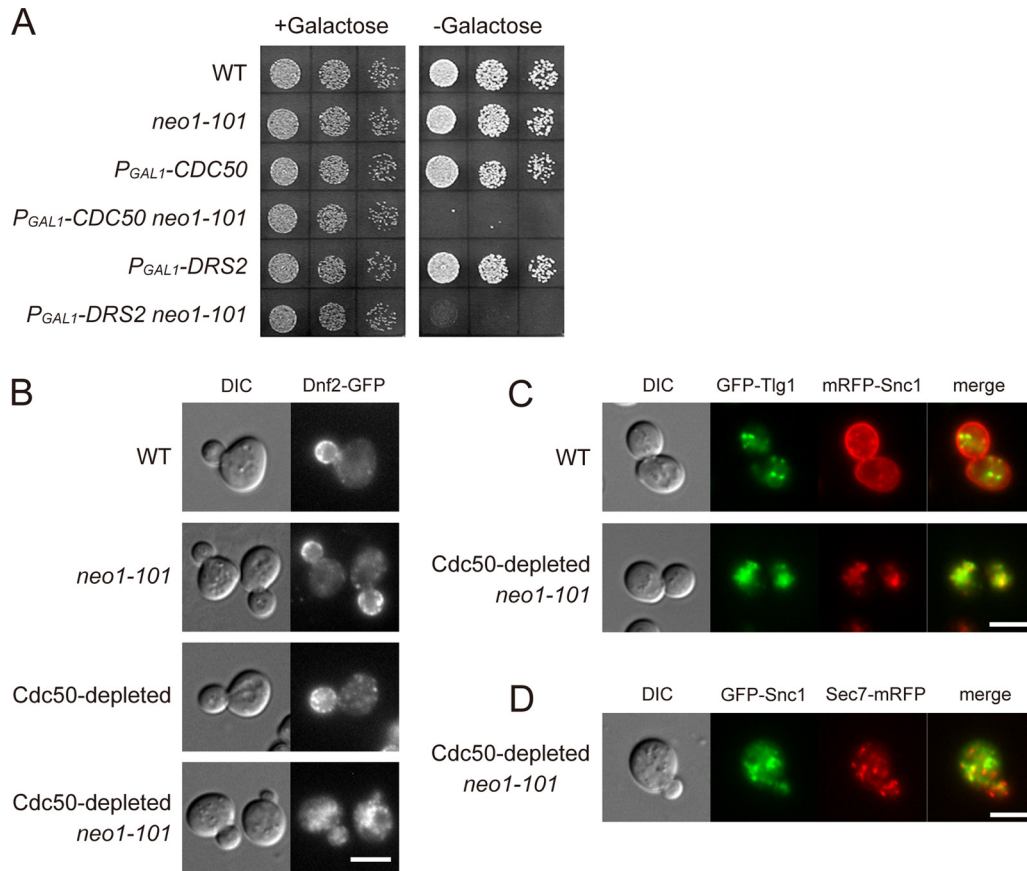


FIG 1 Cdc50p- or Drs2p-depleted *neo1-101* cells exhibit defects in growth and endocytic recycling. (A) Synthetic growth defects between *CDC50* or *DRS2* depletion and *neo1-101*. Cells were grown to early log phase in YPGA, washed, and adjusted at a concentration of 8.0×10^5 cells/ml. Then, 4- μ l drops of 5-fold serial dilutions were spotted onto plates containing galactose (Cdc50p-expressed) or glucose (Cdc50p-depleted), followed by incubation at 30°C for 1 day. The strains were YKT1066 (WT; wild type), YKT1781 (*neo1-101*), YKT1782 (*P_{GAL1}-CDC50*), YKT1783 (*P_{GAL1}-CDC50 neo1-101*), YKT1629 (*P_{GAL1}-DRS2*), and YKT1784 (*P_{GAL1}-DRS2 neo1-101*). (B) Localization of Dnf2p-GFP to abnormal intracellular membranes in the Cdc50p-depleted *neo1-101* mutant. Cells were grown in YPDA medium at 30°C for 12 h, followed by microscopic examination. The strains were YKT1785 (*DNF2-GFP*), YKT1786 (*neo1-101 DNF2-GFP*), YKT1787 (*P_{GAL1}-CDC50 DNF2-GFP*), and YKT1788 (*P_{GAL1}-CDC50 neo1-101 DNF2-GFP*). (C) Colocalization of GFP-Tlg1p and mRFP-Snc1p to membrane structures in Cdc50p-depleted *neo1-101* cells. Cells harboring pRS416-GFP-TLG1 (pKT1488) were grown in SDA-U medium at 30°C for 12 h. The strains were YKT1777 (*mRFP-SNC1*) and YKT1789 (*P_{GAL1}-CDC50 neo1-101 mRFP-SNC1*). Images were merged to compare the two signal patterns. (D) The GFP-Snc1p-containing structures are independent of Sec7p-mRFP. Cells carrying pRS416-GFP-SNC1 (pKT1443) were grown in SDA-U medium at 30°C for 12 h. The strain was YKT1790 (*P_{GAL1}-CDC50 neo1-101 SEC7-mRFP*). Bars, 5 μ m.

Dnf1/2p, and Crf1p-Dnf3p had redundant roles in the early endosome to TGN recycling pathway (7), we examined whether the *neo1-101* mutation aggravated the recycling defect in Cdc50p-depleted cells. Dnf2p, which is mainly localized to polarized growth sites of the plasma membrane (8, 9, 36), is recycled from the plasma membrane via the early endosome to the TGN (37). The *neo1-101* mutant cells exhibited normal polarized localization of Dnf2p-GFP at a bud or a cytokinesis site (99%, $n = 143$ budded cells) like wild-type cells (99%, $n = 145$) (Fig. 1B). In the Cdc50p-depleted cells in which Cdc50p was partially depleted for 12 h in the presence of glucose, Dnf2p-GFP was internally accumulated in some cells, but most of the cells still exhibited polarized Dnf2p-GFP (90%, $n = 122$), as reported previously for GFP-Snc1p (18). In contrast, in the Cdc50p-depleted *neo1-101* mutant, only 8% ($n = 127$) of the cells exhibited polarized Dnf2p-GFP, and the remaining 92% accumulated Dnf2p-GFP in internal structures that seemed to be early endosome-derived abnormal membranes.

To confirm these results, we examined other cargos transported through this pathway. A v-SNARE Snc1p, involved in the

fusion of Golgi-derived secretory vesicles with the plasma membrane, is recycled through the endocytic recycling pathway (38). Tlg1p, an essential t-SNARE mediating fusion of endosome-derived vesicles with the TGN, is recycled between the early endosome and the TGN (39, 40). In wild-type cells, mRFP-Snc1p was localized to polarized plasma membrane sites such as Dnf2p-GFP, whereas GFP-Tlg1p was observed as internal punctate structures reminiscent of endosomal/TGN membranes (Fig. 1C). In the Cdc50p-depleted *neo1-101* mutant, both mRFP-Snc1p and GFP-Tlg1p were localized to internal enlarged compartments (82%, $n = 124$). These compartments were independent of a TGN marker Sec7p-mRFP (Fig. 1D), suggesting that they were early endosome-derived membranes. These results suggest that combination of *cdc50* and *neo1-101* mutations caused the synthetic defect in the retrieval pathway from the early endosome to the TGN.

Overexpression of the phosphatidylserine synthase gene *CHO1* suppresses the endocytic recycling defects in the Cdc50p-depleted *neo1-101* mutant. To obtain a clue to flippase functions, we isolated multicopy suppressors of the synthetic growth defect

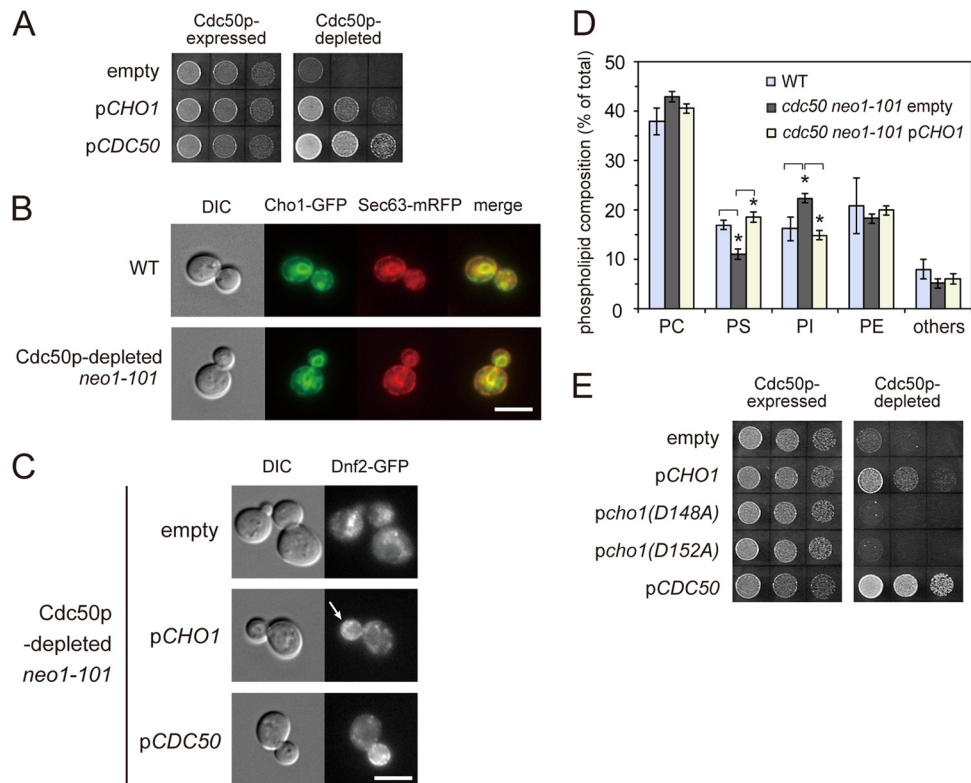


FIG 2 Overexpression of *CHO1* suppresses defects in growth and endocytic recycling of Cdc50p-depleted *neo1[hyphen]101* cells. (A) Suppression of the growth defects. Cells were grown to early log phase in SGA-U medium, and cell growth was examined at 30°C for 1 day as in Fig. 1A with an initial cell concentration of 1.0×10^7 cells/ml. The strains were as follows (abbreviations used in the figure are indicated in brackets): YKT1650 (*P_{GALI}-CDC50 neo1-101*) carrying YEp24 [empty], YEp24-*CHO1* (pKT1753) [*pCHO1*], or YEplac195-*CDC50* (pKT1263) [*pCDC50*]. (B) Localization of the overproduced Cho1p-GFP to the ER membrane. Cells harboring YEplac195-*CHO1*-GFP (pKT2112) were grown in SDA-U medium at 30°C for 12 h. The strains were YKT1871 (*SEC63-mRFP*) and YKT1872 (*P_{GALI}-CDC50 neo1-101 SEC63-mRFP*). Bar, 5 μ m. (C) Suppression of the defects in endocytic recycling of Dnf2p-GFP. Localization of Dnf2p-GFP was examined in the cells grown in SDA-U medium at 30°C for 12 h to deplete Cdc50p. The strains were YKT1788 (*P_{GALI}-CDC50 neo1-101 DNF2-GFP*) carrying the same plasmids as in panel A. Arrows indicate that Dnf2p-GFP is localized to polarized plasma membrane sites, including the bud or the cytokinesis site. Bar, 5 μ m. (D) PS is increased by overexpression of *CHO1*. The cells described in panel A carrying YEp24 (empty) or YEp24-*CHO1* (*pCHO1*) were labeled with 32 P during Cdc50p depletion in SDA-U medium at 30°C for 12 h. Wild-type cells (YKT1066) carrying YEp24 were similarly cultured and 32 P labeled as a control. Phospholipids were extracted, separated, and quantified as described in Materials and Methods. The data represent percentages of total phospholipids with means \pm the standard deviations of three independent experiments. Asterisks indicate a significant difference in the Student *t* test (*, $P < 0.05$). PC, phosphatidylcholine; PI, phosphatidylinositol. (E) Failure of catalytically inactive *cho1* mutant genes to suppress the growth defect. Cells were grown to early log phase in SGA-U medium, and cell growth was examined at 30°C for 1 day as in Fig. 1A with an initial cell concentration of 2.0×10^6 cells/ml. The strains were YKT1872 (*P_{GALI}-CDC50 neo1-101*) carrying YEplac195 (empty), YEplac195-*CHO1* (pKT2111, *pCHO1*), YEplac195-*cho1*(D148A) [pKT2114, *pcho1*(D148A)], YEplac195-*cho1*(D152A) [pKT2115, *pcho1*(D152A)], or YEplac195-*CDC50* (pKT1263, *pCDC50*).

of the Cdc50p-depleted *neo1-101* mutant. *CHO1*, encoding the unique phosphatidylserine synthase in yeast, was isolated (Fig. 2A). Cho1p catalyzes the synthesis of PS from CDP-DAG and serine in the ER (41). To confirm that the overexpressed Cho1p was normally localized to the ER membrane, we constructed the *CHO1*-GFP allele. *CHO1*-GFP was functional, because it complemented the choline auxotrophy and the cold-sensitive growth of the *cho1* Δ mutant (data not shown). The Cho1p-GFP overexpressed from a multicopy plasmid was colocalized with an ER marker Sec63p-mRFP (42) in the Cdc50p-depleted *neo1-101* mutant, as well as in the wild type (Fig. 2B), indicating that the overexpressed Cho1p-GFP was normally localized to the ER. We confirmed that Cho1p-GFP was overexpressed in these strains, because the Cho1p-GFP signal was undetectable under the same condition in a strain expressing Cho1p-GFP from its genomic locus (data not shown).

We examined whether the *CHO1* overexpression also sup-

pressed the recycling defect of Dnf2p-GFP in the Cdc50p-depleted *neo1-101* mutant. When Cdc50p in the *neo1-101* mutant was depleted for 12 h in the glucose-containing synthetic medium (SDA-U), Dnf2p-GFP was polarized in 13% ($n = 142$ budded cells) of the cells, which was slightly higher compared to cells grown in YPDA rich medium (8%, Fig. 1B). The *CHO1* overexpression increased the cells with polarized Dnf2p-GFP to 36% ($n = 140$) (Fig. 2C). This partial suppression was consistent with the partial suppression of the growth defect. Because it was previously shown that *CHO1* overexpression increased cellular PS levels (43), these results suggest that the endocytic recycling of Dnf2p-GFP was restored by increased PS.

To confirm that PS content was increased in the Cdc50p-depleted *neo1-101* mutant by *CHO1* overexpression, we analyzed phospholipid composition in the cells grown under the same condition as in Fig. 2C. Interestingly, we noticed that PS content was decreased from $17.0\% \pm 0.9\%$ of the wild type to $11.1\% \pm 1.9\%$ in

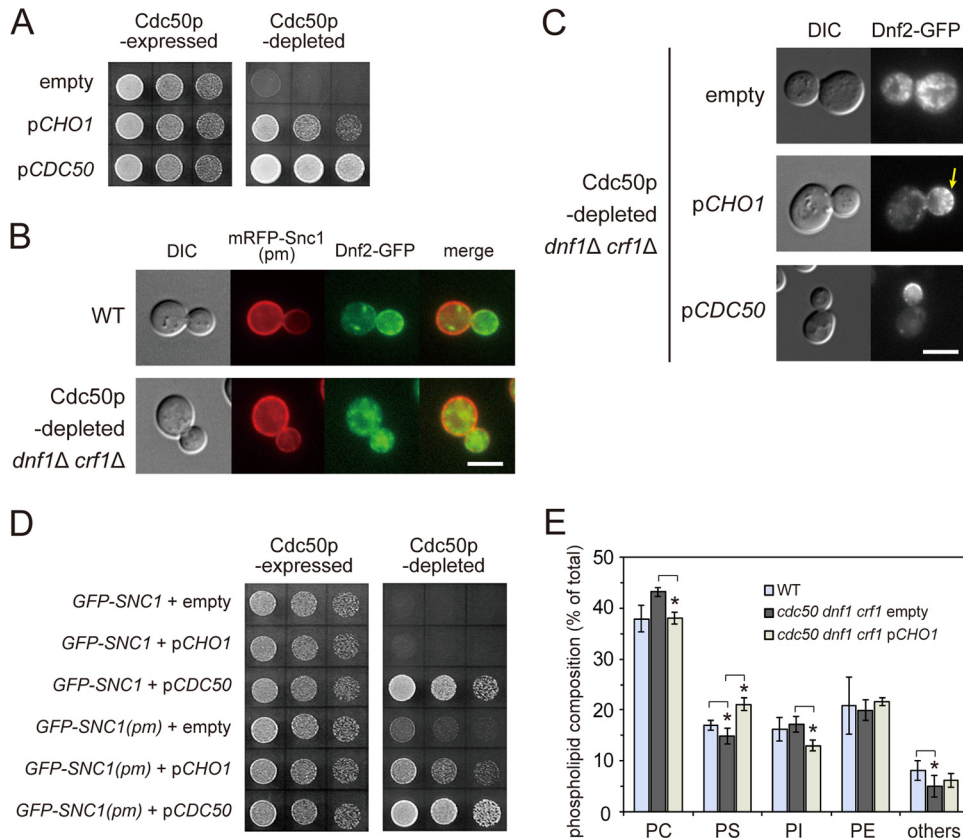


FIG 3 Overexpression of *CHO1* suppresses defects in growth and endocytic recycling of the Cdc50p-depleted *dnf1Δ crf1Δ* mutant. (A) Suppression of the growth defects. Cells were grown to early log phase in SGA-U medium, and cell growth was examined at 25°C for 2 days as in Fig. 1A with an initial cell concentration of 2.0×10^6 cells/ml. The strains were as follows (abbreviations used in the figure are indicated in brackets): YKT1529 ($P_{GALI}-CDC50$ *dnf1Δ crf1Δ*) carrying YEep24 [empty], YEep24-CHO1 (pKT1753) [p*CHO1*], or YEplac195-CDC50 (pKT1263) [p*CDC50*]. (B) Localization of Dnf2p-GFP to intracellular membranes in the Cdc50p-depleted *dnf1Δ crf1Δ* mutant. Localization of Dnf2p-GFP and mRFP-Snc1(pm) was examined in the cells grown in SDA-U medium at 30°C for 12 h to deplete Cdc50p. Images were merged to compare the two signal patterns. The strains were YKT1785 (*DNF2-GFP*) and YKT1791 ($P_{GALI}-CDC50$ *dnf1Δ crf1Δ DNF2-GFP*) carrying pRS416-mRFP-SNC1(pm) (pKT1964). Bar, 5 μ m. (C) Suppression of the defects in endocytic recycling of Dnf2p-GFP. Localization of Dnf2p-GFP was examined in the cells grown as in panel B. The strains were YKT1791 ($P_{GALI}-CDC50$ *dnf1Δ crf1Δ DNF2-GFP*) carrying the same plasmids as in panel A. Arrows indicate that Dnf2p-GFP is localized to the polarized plasma membrane sites. Bar, 5 μ m. (D) GFP tagging of Snc1p, but not of Snc1p(pm), inhibits the suppression of growth defects by *CHO1* overexpression in the Cdc50p-depleted *dnf1Δ crf1Δ* mutant. Cell growth was examined as in panel A at 25°C for 2 days with initial cell concentration of 8.0×10^5 cells/ml. The strains were YKT1792 ($P_{GALI}-CDC50$ *dnf1Δ crf1Δ GFP-SNC1*) and YKT1793 [$P_{GALI}-CDC50$ *dnf1Δ crf1Δ GFP-SNC1(pm)*] carrying the plasmids as in panel A. (E) Increase in PS by overexpression of *CHO1*. The phospholipid content in the wild type and the strains described in panel A carrying YEep24 [empty] or YEep24-CHO1 (pKT1753) [p*CHO1*] was analyzed as in Fig. 2D, including statistical analysis.

the Cdc50p-depleted *neo1-101* mutant, whereas PI content was increased from $16.2\% \pm 2.4\%$ to $22.4\% \pm 0.7\%$ (Fig. 2D). The molecular basis for these phospholipid changes is currently unclear, but this seems to be specific to the Cdc50p-depleted *neo1-101* mutant, because these changes were subtle (PS) or not observed (PI) in the Cdc50p-depleted *dnf1Δ crf1Δ* mutant (Fig. 3E). Overexpressed *CHO1* resulted in 1.7-fold increase of PS content (from $11.1\% \pm 1.9\%$ to $18.6\% \pm 0.6\%$) in the Cdc50p-depleted *neo1-101* mutant (Fig. 2D). In contrast, the phosphatidylinositol (PI) level was decreased from $22.4\% \pm 0.7\%$ to $14.9\% \pm 0.8\%$ by *CHO1* overexpression, probably because CDP-DAG is also a precursor for PI synthesis (44). Because the suppression was dependent on a remaining flippase (see below), increase of PS, a known substrate of flippases, seems to be responsible for the suppression.

To confirm that the suppression is dependent on the enzymatic activity of Cho1p, we examined catalytically inactive mutants of Cho1p. The CDP-alcohol phosphotransferase motif was previously suggested as a catalytic site of the enzymes, including Cho1p

that catalyze the synthesis of a phospholipid by the displacement of CMP from a CDP-alcohol by a second alcohol to form a phosphoester bond. Two aspartic acid residues in this motif, Asp131 and Asp135, were shown to be essential for the catalytic activity of yeast cholinephosphotransferase (Cpt1p) (45). The corresponding residues in Cho1p, Asp148 and Asp152, were replaced with alanine to form Cho1p(D148A) and Cho1p(D152A), respectively. As expected, neither *cho1(D148A)* nor *cho1(D152A)* complemented the choline auxotrophy and the cold-sensitive growth of the *cho1Δ* mutant (data not shown). As shown in Fig. 2E, overexpression of these *cho1* mutant genes did not suppress the growth defect of the Cdc50p-depleted *neo1-101* mutant. We confirmed that both the overexpressed Cho1p(D148A)-GFP and Cho1p(D152A)-GFP were normally localized to the ER as Cho1p-GFP was (data not shown).

The *CHO1* overexpression also suppresses the endocytic recycling defects in the Cdc50p-depleted *dnf1Δ crf1Δ* mutant. To examine whether the suppression was specific to *neo1-101*, we

overexpressed *CHO1* in the Cdc50p-depleted *dnf1Δ crf1Δ* mutant in which Dnf2p-GFP could be also used as a marker for endocytic recycling. As shown in Fig. 3A, the *CHO1* overexpression suppressed the growth defect in the Cdc50p-depleted *dnf1Δ crf1Δ* mutant. In this mutant in which Cdc50p was depleted for 12 h, Dnf2p-GFP was accumulated in intracellular membranes, whereas mRFP-Snc1p(pm), a mutant of Snc1p, was localized to the plasma membrane (Fig. 3B). mRFP-Snc1p(pm) is normally transported to the plasma membrane by the exocytosis pathway but is not endocytosed due to its defects in endocytosis (38). Thus, these results suggest that the Cdc50p-depleted *dnf1Δ crf1Δ* mutant is defective in the endocytic recycling pathway, but not in the exocytosis pathway, and that Dnf2p-GFP was accumulated in early endosome-derived membranes. In the Cdc50p-depleted *dnf1Δ crf1Δ* cells, Dnf2p-GFP was localized to the plasma membrane only in 9% of the cells ($n = 107$ budded cells), whereas it increased to 59% when *CHO1* was overexpressed ($n = 137$) (Fig. 3C). These results suggest that the *CHO1* overexpression partially restored endocytic recycling of Dnf2p-GFP in the Cdc50p-depleted *dnf1Δ crf1Δ* mutant.

We also examined whether the *CHO1* overexpression restored endocytic recycling of GFP-Snc1p in the Cdc50p-depleted *dnf1Δ crf1Δ* cells. However, interestingly, the expression of *GFP-SNC1* inhibited the suppression of growth defects by the *CHO1* overexpression (Fig. 3D). Consistently, endocytic recycling of GFP-Snc1p was not restored by the *CHO1* overexpression either (data not shown). This inhibitory effect was not observed with GFP-Snc1p(pm) (Fig. 3D). Since Snc1p is a cargo of a vesicle formed from early endosomes, these results may suggest that GFP-tagging of Snc1p interferes with some step in vesicle formation, which is promoted by PS increase.

We confirmed that PS content was increased from $14.2\% \pm 1.6\%$ to $20.4\% \pm 0.2\%$ in the Cdc50p-depleted *dnf1Δ crf1Δ* mutant by *CHO1* overexpression, as in the Cdc50p-depleted *neo1-101* mutant (Fig. 3E). Unexpectedly, a slight decrease in the PC level was observed from $43.0\% \pm 1.1\%$ to $38.4\% \pm 1.5\%$ for an unknown reason. A previous study showed that deletion of *PEM2* involved in PC synthesis decreased PC content from 41 to 37% (46). We examined whether the *pem2Δ* mutation suppressed the growth defect in the Cdc50p-depleted *dnf1Δ crf1Δ* mutant, but it did not (data not shown), suggesting that the PC decrease was not responsible for the suppression. Taken together, these results suggest that the defects of growth and endocytic recycling in flippase mutants could be suppressed by PS increase.

Suppression by PS increase seems to be dependent on a remaining flippase. Our results suggest that increase of PS promotes vesicle formation from early endosomes in the flippase mutants. One possible mechanism is that increased PS is used by a remaining flippase to increase efficiency of flippase-mediated vesicle formation, whereas the other possibility is that PS in the outer leaflet of endosomal membranes is sufficient for vesicle formation by itself (e.g., PS recruits vesicle coat proteins). If the suppression is dependent on a flippase, it would not occur in the absence of flippases. We overexpressed *CHO1* in the Cdc50p-depleted *lem3Δ crf1Δ* mutant in which Drs2p, Dnf1p, Dnf2p, and Dnf3p are not functional, but *CHO1* weakly suppressed the growth defect (Fig. 4A). We reasoned that Neo1p might promote vesicle formation with increased PS in this mutant because Neo1p functioned with Drs2p in the endocytic recycling pathway as shown in Fig. 1. In fact, overexpression of *NEO1* suppressed the growth defect of the

Cdc50p-depleted *lem3Δ crf1Δ* mutant, and co-overexpression of *CHO1* and *NEO1* enhanced this suppression (Fig. 4A). Then, we wanted to examine whether *CHO1* overexpression would suppress the growth defect in the Cdc50p- and Neo1p-depleted *lem3Δ crf1Δ* mutant. However, *CHO1* overexpression did not suppress the growth defect of even the Neo1p-depleted single mutant (Fig. 4B). This may be because Neo1p is involved in various cell functions other than the endocytic recycling pathway, including retrograde transport from the Golgi bodies to the ER (10) and membrane trafficking within the endosomal/Golgi system (11). Consistently, the growth defect of Neo1p-depleted cells was not suppressed by the overexpression of *CDC50/DRS2*, *CDC50/DRS2* and *CHO1*, or *LEM3/DNF1* (Fig. 4B).

We next examined the *neo1-101* allele, which seems to be specifically defective in the endocytic recycling pathway. The growth defect of the Cdc50p-depleted *neo1-101* mutant was suppressed by overexpression of *LEM3/DNF1*, as well as *CHO1* (Fig. 4C). In addition, the suppression was enhanced by co-overexpression of *LEM3/DNF1* and *CHO1*. Dnf1p-GFP was normally localized to polarized plasma membrane sites as Dnf2p-GFP was, but in the Cdc50p-deleted *neo1-101* mutant, Dnf1p-GFP was localized to endosomal membranes in which mRFP-Snc1p was accumulated (Fig. 4D). These results suggest that overexpressed Lem3p-Dnf1p supported vesicle formation from early endosomes in the Cdc50p-depleted *neo1-101* mutant and that this vesicle formation was enhanced by PS increase.

Finally, the growth defect in the Cdc50p-depleted *neo1-101 lem3Δ crf1Δ* mutant was not suppressed by overexpression of *CHO1* (Fig. 4E). Thus, we concluded that the suppression of flippase mutations by increased PS was mediated by a remaining flippase.

PS is present in the cytoplasmic leaflet of early endosome membranes even in the absence of flippases. If PS in the cytoplasmic leaflet of early endosome membranes plays a direct role in vesicle formation, PS may not be found in the cytoplasmic leaflet of endosomal membranes that are accumulated in the flippase mutants. Distribution of PS in the cytoplasmic leaflet of the plasma membrane and internal membranes could be monitored with GFP-Lact-C2, the GFP-fused C2 domain of lactadherin, which specifically binds to PS (29).

In wild-type cells, GFP-Lact-C2 was exclusively localized to the plasma membrane, and no intracellular localization was observed, as reported previously (Fig. 5A) (29, 47). In contrast, in the Cdc50p-depleted *dnf1Δ crf1Δ* mutant, GFP-Lact-C2 was also localized to endosomal membranes merged with mRFP-Snc1p (94%, $n = 100$). This GFP-Lact-C2 signal was not observed with a mutant version of GFP-Lact-C2, GFP-Lact-C2-AAA, which does not bind to PS (29). We confirmed that expression of GFP-Lact-C2 did not affect the PS content in the Cdc50p-depleted *dnf1Δ crf1Δ* cells (Fig. 5B). Because it was possible that the PS in the cytoplasmic leaflet resulted from PS flipping by remaining flippases, including Lem3p-Dnf2p and Neo1p, we examined the localization of GFP-Lact-C2 in the mutant in which all known flippases are not functional, that is, the Cdc50p- and Neo1p-depleted *lem3Δ crf1Δ* mutant. GFP-Lact-C2 was again localized to the mRFP-Snc1p-containing membranes (98%, $n = 122$) (Fig. 5C), although this mutant seems to accumulate TGN membranes in addition to endosomal membranes due to possible inhibition of the exocytosis pathway (our unpublished results).

These results seem to be consistent with the expected transbi-

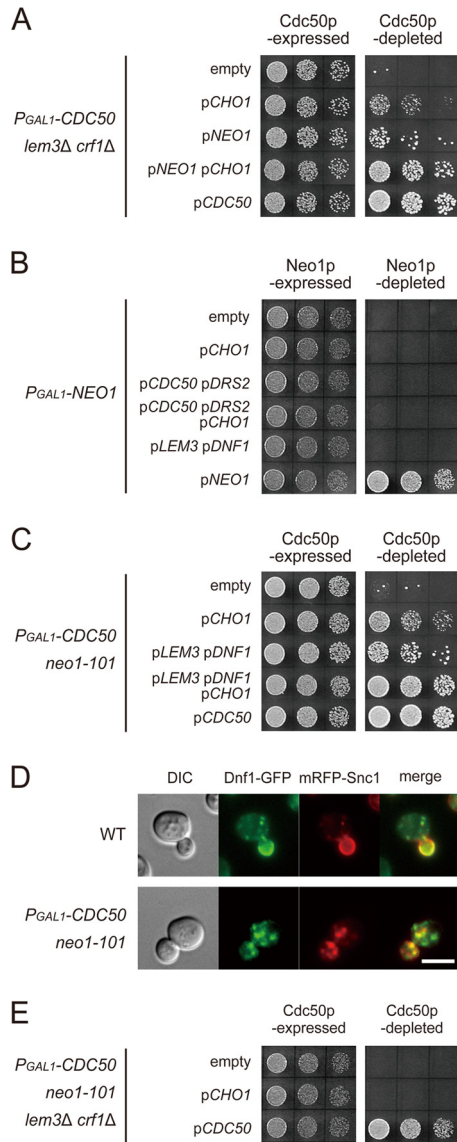


FIG 4 Suppression by the *CHO1* overexpression is dependent on a remaining flippase. (A) Suppression of the growth defect in the Cdc50p-depleted *lem3Δ crf1Δ* mutant by *CHO1* and/or *NEO1* overexpression. Cells were grown to early log phase in SG-LU medium, and cell growth was examined at 30°C for 1 day as in Fig. 1A with an initial cell concentration of 4.0×10^6 cells/ml. The strains were as follows (abbreviations used in the figure are indicated in brackets): YKT1513 (*P_{GALI}-CDC50 lem3Δ crf1Δ*) carrying pRS425 and YEep24 [empty], pRS425 and YEep24-CHO1 (pKT1753) [p*CHO1*], pRS425-NEO1 (pKT1788) and YEep24 [p*NEO1*], pRS425-NEO1 and YEep24-CHO1 [p*NEO1* p*CHO1*], and pRS425 and YEplac195-CDC50 (pKT1263) [p*CDC50*]. (B) Growth defects in the Neo1p-depleted mutant are not suppressed by overexpression of either *CHO1* or other flippases. Cells were grown to early log phase in SGA-UW medium, and cell growth was examined at 30°C for 1 day as in Fig. 1A with an initial cell concentration of 8.0×10^5 cells/ml. The strains were as follows (abbreviations used in the figure are indicated in brackets): YKT1660 (*P_{GALI}-NEO1*) carrying YEplac112 and YEplac195 [empty], YEplac112-CHO1 (pKT2097) and YEplac195 [p*CHO1*], YEplac112 and YEplac195-DRS2-CDC50 (pKT1607) [p*CDC50* p*DRS2*], YEplac112-CHO1 and YEplac195-DRS2-CDC50 [p*CHO1* p*CDC50* p*DRS2*], YEplac112-LEM3 (pKT2098) and YEplac195-DNF1 (pKT1602) [p*LEM3* p*DNF1*], and YEplac112 and YEplac195-NEO1 (pKT1469) [p*NEO1*]. (C) Suppression of the growth defect in the Cdc50p-depleted *neo1-101* mutant by *CHO1* and/or *LEM3/DNF1* overexpression. Cells were grown to early log phase in SG-LWU medium, and cell growth was examined at 30°C for 1 day as in Fig. 1A with

layer distribution of PS in early endosomes: PS enriched in the cytoplasmic leaflet of the plasma membrane would be exposed on the cytoplasmic leaflet of early endosomes after endocytosis and vesicle fusion with early endosomes unless PS is actively transported to the luminal leaflet (flopped) after endocytosis. It was previously shown that PS was actually present in the cytoplasmic leaflet of endocytic vesicles in yeast (48). In wild-type cells, however, no intracellular structures were visualized with GFP-Lact-C2 (Fig. 5A), suggesting that PS is not abundant in the cytoplasmic leaflet of normal early endosomes. While yeast early endosomes are poorly characterized organelles with no specific marker protein identified, they may be too small to be visualized with GFP-Lact-C2 or PS in the cytoplasmic leaflet may be removed by efficient vesicle formation from early endosomes in wild-type cells.

Our results suggest that the mere presence of PS in the cytoplasmic leaflet would not be enough for vesicle formation. Thus, we propose that PS has to be flipped by flippases from the luminal to the cytoplasmic leaflet when a vesicle is formed (e.g., PS flipping is coupled with vesicle formation). This luminal PS in early endosomes, which would not be supplied by endocytic vesicles, may be delivered by vesicle transport from TGN membranes.

PS is not essential for the endocytic recycling pathway. We next examined whether PS is essential for the early endosome to TGN retrieval pathway. Deletion of *CHO1* completely eliminates PS synthesis and depletes PS from these strains (49). In *cho1Δ* cells, GFP-Snc1p was normally localized to polarized plasma membrane sites as in wild-type cells (Fig. 6A), suggesting that the endocytic recycling pathway was not largely affected in *cho1Δ* cells. GFP-Snc1p(pm) was also exclusively localized at the plasma membrane in *cho1Δ* cells as in wild-type cells, a finding consistent with a previous report that protein transport and processing in the secretory pathway was normal in the *cho1Δ* mutant (12). In *cho1Δ* cells, the AP-1 $\beta 1$ subunit, Apl2p-GFP, was localized to dotty structures that are endosomal/TGN membranes as in wild-type cells (50), indicating that PS is not essential for recruitment of AP-1 to these membranes. Taken together, these results suggest that PS is dispensable for the endocytic recycling pathway, as well as for the secretory pathway.

To examine the impact of PS depletion on the Cdc50p-Drs2p function, we analyzed the *cdc50Δ cho1Δ* double mutant. As reported previously for the *drs2Δ cho1Δ* mutant (12), the *cdc50Δ*

an initial cell concentration of 4.0×10^6 cells/ml. The strains were as follows (abbreviations used in the figure are indicated in brackets): YKT1650 (*P_{GALI}-CDC50 neo1-101*) carrying YEplac181, YEplac195, and YEplac112 [empty], YEplac181, YEplac195, and YEplac112-CHO1 (pKT2097) [p*CHO1*], YEplac181-LEM1 (pKT1340), YEplac195-DNF1 (pKT1602), and YEplac112 [p*LEM3* p*DNF1*], YEplac181-LEM1, YEplac195-DNF1, and YEplac112-CHO1 [p*LEM3* p*DNF1* p*CHO1*], and YEplac181, YEplac195, and YCplac22-CDC50 (pKT1264) [p*CDC50*]. (D) Colocalization of Dnf1p-GFP with mRFP-Snc1p in early endosomal membranes in the Cdc50p-depleted *neo1-101* mutant. Localization of Dnf1p-GFP and mRFP-Snc1p was examined in the cells grown in SDA-U medium at 30°C for 12 h to deplete Cdc50p. The strains were YKT1797 (*DNF1-GFP*) and YKT1798 (*P_{GALI}-CDC50 neo1-101 DNF1-GFP*) carrying pRS416-mRFP-SNC1 (pKT1563). Bar, 5 μ m. (E) Growth defects in the Cdc50p-depleted *neo1-101 lem3Δ crf1Δ* mutant are not suppressed by *CHO1* overexpression. Cells were grown to early log phase in SGA-U medium, and cell growth was examined at 30°C for 1 day as in Fig. 1A with initial cell concentration of 8.0×10^5 cells/ml. The strains were as follows (abbreviations used in the figure are indicated in brackets): YKT1796 (*P_{GALI}-CDC50 neo1-101 lem3Δ crf1Δ*) carrying YEep24 [empty], YEep24-CHO1 (pKT1753) [p*CHO1*], and YEplac195-CDC50 (pKT1263) [p*CDC50*].

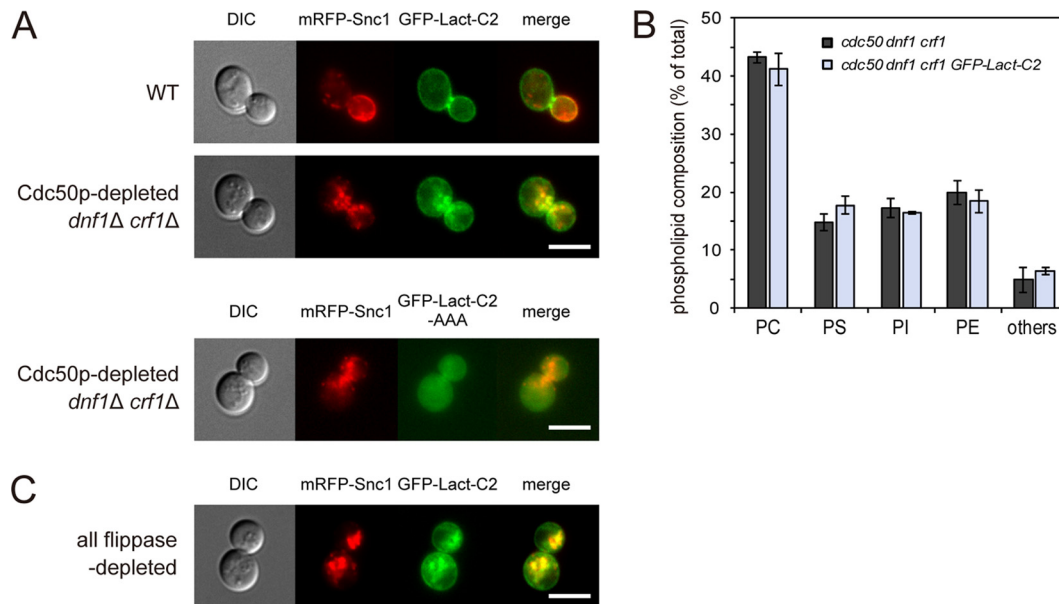


FIG 5 GFP-Lact-C2 is localized to early endosomal membranes accumulated in the flippase mutants. (A) Colocalization of GFP-Lact-C2 with mRFP-Snc1p on endosomal membranes in the Cdc50p-depleted *dnf1Δ crf1Δ* mutant. Localization of mRFP-Snc1p and GFP-Lact-C2 or GFP-Lact-C2-AAA was examined in the cells grown in SDA-U medium at 30°C for 12 h to deplete Cdc50p. The strains were YKT1799 (*GFP-Lact-C2*) and YKT1801 (*P_{GALI}-CDC50 dnf1Δ crf1Δ GFP-Lact-C2*) carrying pRS416-mRFP-SNC1 (pKT1563) and YKT1801 (*P_{GALI}-CDC50 dnf1Δ crf1Δ GFP-Lact-C2-AAA mRFP-SNC1*). (B) PS content is not affected by expression of GFP-Lact-C2 in the Cdc50p-depleted *dnf1Δ crf1Δ* mutant. The phospholipid content was analyzed as in Fig. 2D. The strains were YKT1529 (*P_{GALI}-CDC50 dnf1Δ crf1Δ*) and YKT1800 (*P_{GALI}-CDC50 dnf1Δ crf1Δ GFP-Lact-C2*). (C) Colocalization of GFP-Lact-C2 with mRFP-Snc1p in the Cdc50p- and Neo1p-deleted *lem3Δ crf1Δ* mutant. Localization of mRFP-Snc1p and GFP-Lact-C2 was examined in the cells grown in SD-L medium at 30°C for 8 h to deplete Cdc50p and Neo1p. The strain was YKT1802 (*P_{GALI}-CDC50 P_{GALI}-NEO1 lem3Δ crf1Δ GFP-Lact-C2*) carrying pRS315-mRFP-SNC1 (pKT1568). Bars, 5 μm.

cho1Δ mutant exhibited a synthetic growth defect (Fig. 6B). This growth defect paralleled the defect in endocytic recycling of Dnf2p-GFP: Dnf2p-GFP was normally polarized in *cho1Δ* cells (83%, $n = 117$ budded cells) and was significantly polarized in Cdc50p-depleted cells (34%, $n = 119$) but not in Cdc50p-depleted *cho1Δ* cells (5%, $n = 104$) (Fig. 6C). In the Cdc50p-depleted *cho1Δ* cells, Dnf2p-GFP was localized to membrane structures that were not colocalized with Sec7p-mRFP (Fig. 6D), suggesting that Cdc50p-Drs2p and Cho1p redundantly function in the endocytic recycling pathway. We concluded that, although PS increase alleviates growth and endocytic recycling defects in flippase mutants and PS is involved in the flippase function, PS is not an essential phospholipid for the flippase-mediated vesicle formation from early endosomes.

Increased PE also alleviates defects in the flippase mutants.

The results described above suggest that, in the *cho1Δ* mutant, phospholipids other than PS are utilized by flippases to promote vesicle formation from early endosomes. Because PE is also a potential substrate of flippases (6, 9, 13), we next examined whether increased PE would suppress the defects in the flippase mutants. *PSD1* and *PSD2* encode phosphatidylserine decarboxylases that catalyze formation of PE from PS. Psd1p is engaged in mitochondrial PE biosynthesis (51, 52), whereas Psd2p is implicated in PE synthesis in endosomal/TGN membranes (53, 54). As shown in Fig. 7A, overexpression of *PSD2* weakly suppressed the growth defect of Cdc50p-depleted *dnf1Δ crf1Δ* cells, as well as Cdc50p-depleted *neo1-101* cells, although this suppression was observed in synthetic (SDA) medium, but not in rich (YPD) medium (data not shown). We confirmed that the total cellular PE content was increased from $18.3\% \pm 1.6\%$ to $22.4\% \pm 1.5\%$ and from

$19.9\% \pm 2.1\%$ to $23.5\% \pm 1.9\%$ by *PSD2* overexpression in the Cdc50p-depleted *neo1-101* and Cdc50p-depleted *dnf1Δ crf1Δ* cells, respectively (Fig. 7B). Consistent with the weak suppression of growth defects, cells with polarized Dnf2p-GFP were increased from $11.5\% \pm 3.0\%$ to $23.0\% \pm 3.2\%$ by *PSD2* overexpression in the Cdc50p-depleted *dnf1Δ crf1Δ* cells (Student *t* test, *, $P < 0.05$, four independent experiments) (data not shown).

We next examined whether PE is required for endocytic recycling of GFP-Snc1p. Although complete depletion of PE results in lethality, the *psd1Δ psd2Δ* mutant is viable, because Dpl1p coding for dihydrosphingosine-1-phosphate lyase permits low levels of PE synthesis (55, 56). In the *psd1Δ psd2Δ* mutant, PE content was markedly decreased to $2.2\% \pm 0.2\%$ from $16.6\% \pm 1.4\%$ in the wild type (Fig. 7C). However, GFP-Snc1p was normally localized to polarized sites in the *psd1Δ psd2Δ* mutant (Fig. 7D). In addition, the *psd1Δ psd2Δ cdc50Δ* mutant did not exhibit synthetic defects in growth and endocytic recycling of GFP-Snc1p (data not shown). These results suggest that the low level of PE does not cause a defect in the flippase-mediated vesicle formation from early endosomes.

Taken together, our results raise the possibility that, in addition to PS, PE could be also utilized by flippases to promote vesicle formation from early endosomes in the early endosome-to-TGN pathway.

DISCUSSION

In this study we demonstrate that an increase in PS caused by the overexpression of *CHO1* alleviates defects in the growth and endocytic recycling of flippase mutants. Many studies using a fluorescence-labeled phospholipid analogue or a lipid-binding peptide have suggested that flippases translocate phospholipids, but it

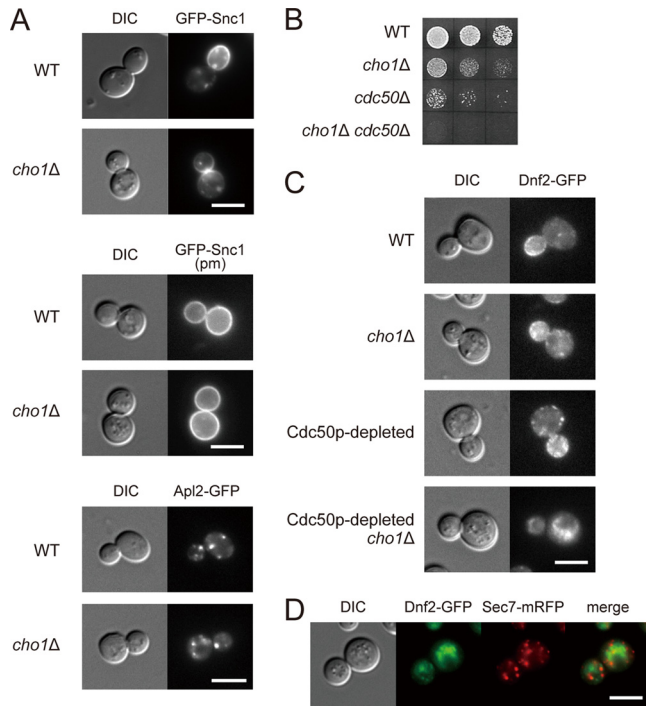


FIG 6 PS is not essential for the endocytic recycling pathway. (A) Localization of GFP-Snc1p, GFP-Snc1p(pm), and Apl2p-GFP in the *cho1Δ* mutant. Cells were grown at 30°C in SDA-U medium supplemented with 2 mM ethanolamine [for GFP-Snc1p and GFP-Snc1p(pm)] or in YPDA medium (for Apl2p-GFP), followed by microscopic examination. The strains were YKT1066 (WT) and YKT1428 (*cho1Δ*) carrying pRS416-GFP-SNC1 (pKT1443) or pRS416-GFP-SNC1(pm) (pKT1444), YKT1642 (*APL2-GFP*), and YKT1803 (*cho1Δ APL2-GFP*). (B) Synthetic growth defects between *cho1Δ* and *cdc50Δ* mutations. Cell growth was examined on YPDA medium as in Fig. 1A at 25°C for 2 days with an initial cell concentration of 4.0×10^6 cells/ml. The strains were YKT1066 (WT), YKT1428 (*cho1Δ*), YKT1507 (*cdc50Δ*), and YKT1804 (*cho1Δ cdc50Δ*). (C) Localization of Dnf2p-GFP in Cdc50p-depleted *cho1Δ* cells. Localization of Dnf2p-GFP was examined in the cells grown in YPDA medium at 30°C for more than 24 h to deplete Cdc50p. The strains were YKT1805 (*DNF2-GFP*), YKT1806 (*cho1Δ DNF2-GFP*), YKT1787 (*P_{GALI}-CDC50 DNF2-GFP*), and YKT1807 (*P_{GALI}-CDC50 cho1Δ DNF2-GFP*). (D) Dnf2p-GFP is not colocalized with Sec7p-mRFP in the Cdc50p-depleted *cho1Δ* mutant. Cells of YKT1808 (*P_{GALI}-CDC50 cho1Δ DNF2-GFP SEC7-mRFP*) were grown and observed as in panel C. Bars, 5 μ m.

needs to be demonstrated that flippases act on endogenous phospholipids. Our results provide genetic evidence for the functional relevance between flippases and endogenous phospholipids.

Neo1p is distinct from other flippases in that it is an essential protein and does not associate with a Cdc50p family member. Isolation and characterization of the *neo1-101* mutant suggested that Neo1p is involved in the endocytic recycling pathway. We previously isolated *NEO1* as a multicopy suppressor of the *cdc50-11 lem3Δ crf1Δ* mutant (7). Although Neo1p has not been demonstrated to possess a flippase activity, these results imply that Neo1p functions as a flippase like other flippases.

Overexpression of *CHO1* caused two opposite effects in the phospholipid content: an increase in PS and a decrease in PI. Although we cannot exclude a possibility that a decrease in PI is involved in the suppression, the increase in PS, a known substrate of flippases, seems to be responsible, because the suppression was dependent on remaining flippases. Thus, it was suggested that increased PS was flipped by the flippases to promote vesicle for-

mation from early endosomes. The *cdc50Δ* mutation exhibited synthetic defects with *cho1Δ*, but not with *psd1Δ psd2Δ*, suggesting that PS is functionally more relevant to flippases than PE. Since PS has been suggested to be a preferable substrate of Drs2p *in vitro* (12, 14), PS seems to be more effective in Drs2p-mediated vesicle formation than other phospholipids. In contrast, it has not been clearly demonstrated that Lem3p-Dnf1/2p flips PS: NBD-labeled PS was still flipped in the *lem3Δ* mutant probably due to an unidentified protein on the plasma membrane (57), and NBD-PS was a less preferred substrate of Dnf1p compared to NBD-PC and NBD-PE (58). However, growth of the *lem3Δ* mutant was clearly sensitive to papuamide B, a cyclic lipopeptide that shows cytotoxicity by binding to PS in biological membranes (59), and this sensitivity was suppressed by the *cho1Δ* mutation (our unpublished results), indicating that PS is exposed on the cell surface in this mutant. These results may suggest that Lem3p-Dnf1/2p flips PS more efficiently than NBD-PS.

Two possible mechanisms could be envisioned regarding how increased PS enhances vesicle formation. One is that flipped PS in the cytoplasmic leaflet recruits adaptor or coat proteins for vesicle formation with its negative charge. PS has been suggested to be an important factor for directing endocytic proteins to the plasma membrane (60). In the *cdc50Δ* and *rcy1Δ* mutants, in which early endosomal membranes are intracellularly accumulated, endocytic proteins were assembled on those membranes, probably in a PS-dependent manner (60, 61). In mammalian cells, PS in recycling endosomes recruited evectin-2 via interaction with the pleckstrin homology (PH) domain (62). However, GFP-Lact-C2 detected PS in the cytoplasmic leaflet of early endosome membranes in flippase mutants. This PS seems to be transported from the plasma membrane through the endocytosis-recycling route (60). These results suggest that the presence of PS in the cytoplasmic leaflet is not sufficient for vesicle formation.

Thus, we favor the other mechanism: PS flipping by a flippase induces a local membrane curvature that assists in vesicle formation (21). Elucidation of how this membrane curvature is harnessed to form a vesicle is the next challenge. Proteins containing an amphipathic lipid packing sensor (ALPS) motif (63) are candidates that recognize the flippase-induced membrane curvature. We previously showed that the Arf1p GTPase activating protein gene *GCS1* genetically interacts with *CDC50* (18) and have recently shown that its ALPS motif is involved in this functional interaction (64). More recently, Gcs1p has been proposed to be an effector that recognizes the membrane curvature induced by Cdc50p-Drs2p through its ALPS motif (65). However, the endocytic recycling defects in the *gcs1Δ* mutant are negligible compared to the *cdc50Δ/drs2Δ* mutant (our unpublished results), indicating that there should be another protein that recognizes the membrane curvature formed by Cdc50p-Drs2p.

Although PS has been suggested to be a preferable substrate of Drs2p *in vitro* (12, 14), the endocytic recycling pathway was not totally dependent on PS. Endocytic recycling was not significantly affected in the *cho1Δ* mutant but severely impaired in the *cho1Δ cdc50Δ* mutant, indicating that Cdc50p-Drs2p has a function(s) in the endocytic recycling pathway in the absence of PS. Cdc50p-Drs2p might perform a flippase-independent function as suggested for mammalian ATP8B1 flippase (66), but another interesting possibility is that Cdc50p-Drs2p flips PE, as suggested previously (6, 13), to form a vesicle in the absence of PS.

Similar to PS, increased PE alleviated the growth defect of the

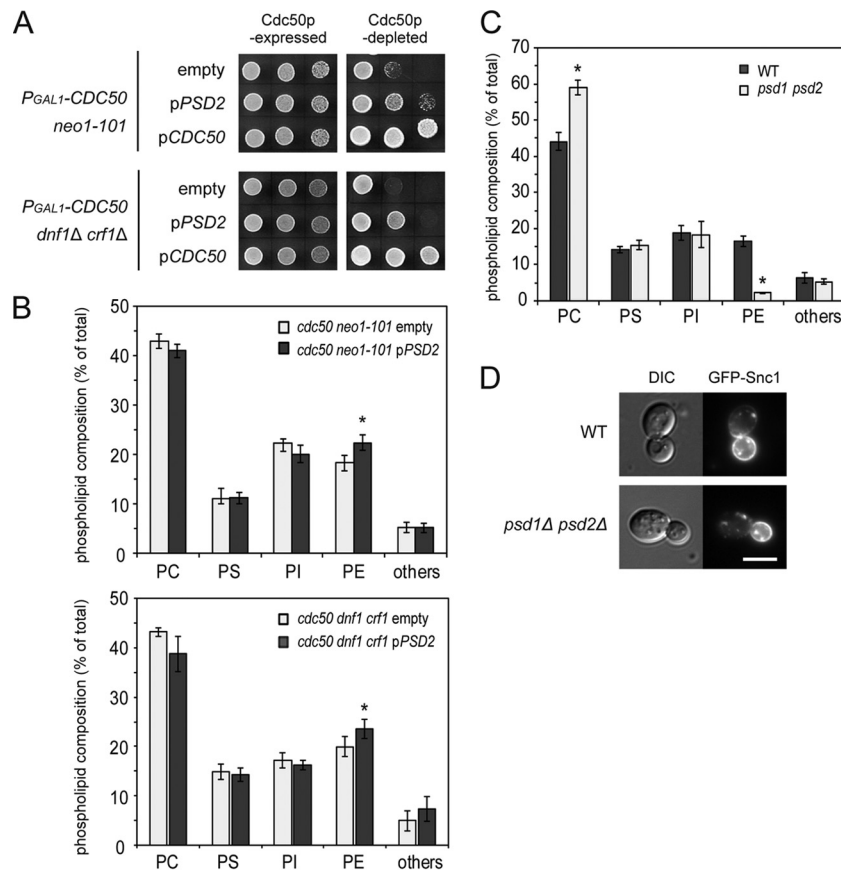


FIG 7 Increased PE also suppresses the growth defects in the Cdc50p-depleted *neo1-101* and Cdc50p-depleted *dnf1Δ crf1Δ* mutants. (A) Suppression by overexpression of *PSD2*. Cell growth was examined on synthetic plate media (SGA-U or SDA-U) as in Fig. 1A at 25°C for 2.5 and 2 days with an initial cell concentration of 2.0×10^6 (Cdc50p-depleted *neo1-101*) and 1.0×10^7 (Cdc50p-depleted *dnf1Δ crf1Δ*) cells/ml, respectively. The strains were as follows (abbreviations used in the figure are indicated in brackets): YKT1650 (*P_{GAL1}-CDC50 neo1-101*) and YKT1529 (*P_{GAL1}-CDC50 dnf1Δ crf1Δ*) carrying YEp24 [empty], YEp352-*PSD2* (pKT2096) [p*PSD2*], or YEplac195-*CDC50* (pKT1263) [p*CDC50*]. (B) PE is increased by overexpression of *PSD2*. The phospholipid content was analyzed as in Fig. 2D. Strains were those carrying YEp24 (empty) and YEp352-*PSD2* (p*PSD2*) in panel A. (C) Decrease in PE in the *psd1Δ psd2Δ* mutant. Cells were grown to early log phase and 32 P-labeled at 30°C in SD medium supplemented with 2 mM choline. The phospholipid content was analyzed as in Fig. 2D, including statistical analysis. An increase in PC was also observed, possibly because cells were grown with 2 mM choline. The strains were YKT1066 (WT) and YKT1809 (*psd1Δ psd2Δ*). (D) Localization of GFP-Snc1p in the *psd1Δ psd2Δ* mutant. Cells were grown at 30°C in SD medium supplemented with 2 mM choline, followed by microscopic examination. The strains were YKT1523 (*GFP-SNC1*) and YKT1810 (*psd1Δ psd2Δ GFP-SNC1*). Bar, 5 μ m.

Cdc50p-depleted *neo1-101* and *dnf1Δ crf1Δ* mutants, which contain Lem3p-Dnf1/2p and Lem3p-Dnf2p, respectively. These flippases may utilize increased PE to form a vesicle because Lem3p-Dnf1/2p has been suggested to translocate a fluorescently labeled PE and PC (9, 15). Interestingly, simultaneous depletion of PS and PE (*cho1Δ* cells grown in SD medium supplemented with 2 mM choline) did not cause an obvious recycling defect (our unpublished results). It is possible that Lem3p-Dnf1/2p also flips PC in the absence of both PS and PE to form a vesicle from early endosomes.

Because both Cdc50p-Drs2p and Lem3p-Dnf1/2p are involved in the endocytic recycling pathway, it seems likely that PE/PC flipping contributes to flippase-mediated vesicle formation, albeit with reduced efficiency compared to PS. This is also consistent with our notion that flippase-mediated vesicle formation is promoted by membrane curvature rather than the chemical or physical properties of a specific phospholipid.

ACKNOWLEDGMENTS

We thank S. Moye-Rowley for yeast strains and plasmids. We thank T. Yamamoto and our coworkers in the Tanaka laboratory for valuable dis-

cussions, T. Sano for construction of *CHO1* plasmids, and Eriko Itoh for technical assistance.

This study was supported by Japan Society for the Promotion of Science KAKENHI grant 21370085.

REFERENCES

1. Lenoir G, Williamson P, Holthuis JC. 2007. On the origin of lipid asymmetry: the flip side of ion transport. *Curr. Opin. Chem. Biol.* 11:654–661. <http://dx.doi.org/10.1016/j.cbpa.2007.09.008>.
2. Sebastian TT, Baldrige RD, Xu P, Graham TR. 2012. Phospholipid flippases: building asymmetric membranes and transport vesicles. *Biochim. Biophys. Acta* 1821:1068–1077. <http://dx.doi.org/10.1016/j.bbalip.2011.12.007>.
3. Tanaka K, Fujimura-Kamada K, Yamamoto T. 2011. Functions of phospholipid flippases. *J. Biochem.* 149:131–143. <http://dx.doi.org/10.1093/jb/mvq140>.
4. Daleke DL. 2007. Phospholipid flippases. *J. Biol. Chem.* 282:821–825. <http://dx.doi.org/10.1074/jbc.R600035200>.
5. van der Mark VA, Elferink RP, Paulusma CC. 2013. P4 ATPases: flippases in health and disease. *Int. J. Mol. Sci.* 14:7897–7922. <http://dx.doi.org/10.3390/ijms14047897>.
6. Saito K, Fujimura-Kamada K, Furuta N, Kato U, Umeda M, Tanaka K. 2004. Cdc50p, a protein required for polarized growth, associates with the Drs2p P-type ATPase implicated in phospholipid translocation in *Saccha-*

- Saccharomyces cerevisiae*. Mol. Biol. Cell 15:3418–3432. <http://dx.doi.org/10.1091/mbc.E03-11-0829>.
7. Furuta N, Fujimura-Kamada K, Saito K, Yamamoto T, Tanaka K. 2007. Endocytic recycling in yeast is regulated by putative phospholipid translocases and the Ypt31p/32p-Rcy1p pathway. Mol. Biol. Cell 18:295–312. <http://dx.doi.org/10.1091/mbc.E06-05-0461>.
 8. Hua Z, Fatheddin P, Graham TR. 2002. An essential subfamily of Drs2p-related P-type ATPases is required for protein trafficking between Golgi complex and endosomal/vacuolar system. Mol. Biol. Cell 13:3162–3177. <http://dx.doi.org/10.1091/mbc.E02-03-0172>.
 9. Pomorski T, Lombardi R, Riezman H, Devaux PF, van Meer G, Holthuis JC. 2003. Drs2p-related P-type ATPases Dnf1p and Dnf2p are required for phospholipid translocation across the yeast plasma membrane and serve a role in endocytosis. Mol. Biol. Cell 14:1240–1254. <http://dx.doi.org/10.1091/mbc.E02-08-0501>.
 10. Hua Z, Graham TR. 2003. Requirement for neo1p in retrograde transport from the Golgi complex to the endoplasmic reticulum. Mol. Biol. Cell 14:4971–4983. <http://dx.doi.org/10.1091/mbc.E03-07-0463>.
 11. Wicky S, Schwarz H, Singer-Krüger B. 2004. Molecular interactions of yeast Neo1p, an essential member of the Drs2 family of aminophospholipid translocases, and its role in membrane trafficking within the endomembrane system. Mol. Cell. Biol. 24:7402–7418. <http://dx.doi.org/10.1128/MCB.24.17.7402-7418.2004>.
 12. Natarajan P, Wang J, Hua Z, Graham TR. 2004. Drs2p-coupled aminophospholipid translocase activity in yeast Golgi membranes and relationship to in vivo function. Proc. Natl. Acad. Sci. U. S. A. 101:10614–10619. <http://dx.doi.org/10.1073/pnas.0404146101>.
 13. Alder-Baerens N, Lisman Q, Luong L, Pomorski T, Holthuis JC. 2006. Loss of P4 ATPases Drs2p and Dnf3p disrupts aminophospholipid transport and asymmetry in yeast post-Golgi secretory vesicles. Mol. Biol. Cell 17:1632–1642. <http://dx.doi.org/10.1091/mbc.E05-10-0912>.
 14. Zhou X, Graham TR. 2009. Reconstitution of phospholipid translocase activity with purified Drs2p, a type-IV P-type ATPase from budding yeast. Proc. Natl. Acad. Sci. U. S. A. 106:16586–16591. <http://dx.doi.org/10.1073/pnas.0904293106>.
 15. Kato U, Emoto K, Fredriksson C, Nakamura H, Ohta A, Kobayashi T, Murakami-Murofushi K, Umeda M. 2002. A novel membrane protein, Ros3p, is required for phospholipid translocation across the plasma membrane in *Saccharomyces cerevisiae*. J. Biol. Chem. 277:37855–37862. <http://dx.doi.org/10.1074/jbc.M205564200>.
 16. Chen CY, Ingram MF, Rosal PH, Graham TR. 1999. Role for Drs2p, a P-type ATPase and potential aminophospholipid translocase, in yeast late Golgi function. J. Cell Biol. 147:1223–1236. <http://dx.doi.org/10.1083/jcb.147.6.1223>.
 17. Gall WE, Geething NC, Hua Z, Ingram MF, Liu K, Chen SI, Graham TR. 2002. Drs2p-dependent formation of exocytic clathrin-coated vesicles *in vivo*. Curr. Biol. 12:1623–1627. [http://dx.doi.org/10.1016/S0960-9822\(02\)01148-X](http://dx.doi.org/10.1016/S0960-9822(02)01148-X).
 18. Sakane H, Yamamoto T, Tanaka K. 2006. The functional relationship between the Cdc50p-Drs2p putative aminophospholipid translocase and the ArfGAP Gcs1p in vesicle formation in the retrieval pathway from yeast early endosomes to the TGN. Cell Struct. Funct 31:87–108. <http://dx.doi.org/10.1247/csf.06021>.
 19. Liu K, Surendhran K, Nothwehr SF, Graham TR. 2008. P4-ATPase requirement for AP-1/clathrin function in protein transport from the *trans*-Golgi network and early endosomes. Mol. Biol. Cell 19:3526–3535. <http://dx.doi.org/10.1091/mbc.E08-01-0025>.
 20. Kelly BT, Owen DJ. 2011. Endocytic sorting of transmembrane protein cargo. Curr. Opin. Cell Biol. 23:404–412. <http://dx.doi.org/10.1016/j.ceb.2011.03.004>.
 21. Graham TR, Kozlov MM. 2010. Interplay of proteins and lipids in generating membrane curvature. Curr. Opin. Cell Biol. 22:430–436. <http://dx.doi.org/10.1016/j.ceb.2010.05.002>.
 22. Rose MD, Winston F, Hieter P. 1990. Methods in yeast genetics: a laboratory course manual. Cold Spring Harbor Laboratory Press, Cold Spring Harbor, NY.
 23. Guthrie C. 1991. Guide to yeast genetics and molecular biology. In Fink GR (ed), Methods in enzymology, vol 194, p 21–37. Academic Press, Inc., San Diego, CA.
 24. Gietz RD, Woods RA. 2002. Transformation of yeast by lithium acetate/single-stranded carrier DNA/polyethylene glycol method. Methods Enzymol. 350:87–96. [http://dx.doi.org/10.1016/S0076-6879\(02\)50957-5](http://dx.doi.org/10.1016/S0076-6879(02)50957-5).
 25. Elble R. 1992. A simple and efficient procedure for transformation of yeasts. Biotechniques 13:18–20.
 26. Longtine MS, McKenzie A, Demarini DJ, Shah NG, Wach A, Brachat A, Philippsen P, Pringle JR. 1998. Additional modules for versatile and economical PCR-based gene deletion and modification in *Saccharomyces cerevisiae*. Yeast 14:953–961. [http://dx.doi.org/10.1002/\(SICI\)1097-0061\(199807\)14:10<953::AID-YEA293>3.0.CO;2-L](http://dx.doi.org/10.1002/(SICI)1097-0061(199807)14:10<953::AID-YEA293>3.0.CO;2-L).
 27. Hachiro T, Yamamoto T, Nakano K, Tanaka K. 2013. Phospholipid flippases Lem3p-Dnf1p and Lem3p-Dnf2p are involved in the sorting of the tryptophan permease Tat2p in yeast. J. Biol. Chem. 288:3594–3608. <http://dx.doi.org/10.1074/jbc.M112.416263>.
 28. Goldstein AL, McCusker JH. 1999. Three new dominant drug resistance cassettes for gene disruption in *Saccharomyces cerevisiae*. Yeast 15:1541–1553. [http://dx.doi.org/10.1002/\(SICI\)1097-0061\(199910\)15:14<1541::AID-YEA476>3.0.CO;2-K](http://dx.doi.org/10.1002/(SICI)1097-0061(199910)15:14<1541::AID-YEA476>3.0.CO;2-K).
 29. Yeung T, Gilbert GE, Shi J, Silvius J, Kapus A, Grinstein S. 2008. Membrane phosphatidylserine regulates surface charge and protein localization. Science 319:210–213. <http://dx.doi.org/10.1126/science.1152066>.
 30. Ho SN, Hunt HD, Horton RM, Pullen JK, Pease LR. 1989. Site-directed mutagenesis by overlap extension using the polymerase chain reaction. Gene 77:51–59. [http://dx.doi.org/10.1016/0378-1119\(89\)90358-2](http://dx.doi.org/10.1016/0378-1119(89)90358-2).
 31. Ma H, Kunes S, Schatz PJ, Botstein D. 1987. Plasmid construction by homologous recombination in yeast. Gene 58:201–216. [http://dx.doi.org/10.1016/0378-1119\(87\)90376-3](http://dx.doi.org/10.1016/0378-1119(87)90376-3).
 32. Botstein D, Falco SC, Stewart SE, Brennan M, Scherer S, Stinchcomb DT, Struhl K, Davis RW. 1979. Sterile host yeasts (SHY): a eukaryotic system of biological containment for recombinant DNA experiments. Gene 8:17–24. [http://dx.doi.org/10.1016/0378-1119\(79\)90004-0](http://dx.doi.org/10.1016/0378-1119(79)90004-0).
 33. Bligh EG, Dyer WJ. 1959. A rapid method of total lipid extraction and purification. Can. J. Biochem. Physiol. 37:911–917. <http://dx.doi.org/10.1139/o59-099>.
 34. Schüller C, Mamnun YM, Wolfger H, Rockwell N, Thorner J, Kuchler K. 2007. Membrane-active compounds activate the transcription factors Pdr1 and Pdr3 connecting pleiotropic drug resistance and membrane lipid homeostasis in *Saccharomyces cerevisiae*. Mol. Biol. Cell 18:4932–4944. <http://dx.doi.org/10.1091/mbc.E07-06-0610>.
 35. Weerheim AM, Kolb AM, Sturk A, Nieuwland R. 2002. Phospholipid composition of cell-derived microparticles determined by one-dimensional high-performance thin-layer chromatography. Anal. Biochem. 302:191–198. <http://dx.doi.org/10.1006/abio.2001.5552>.
 36. Nakano K, Yamamoto T, Kishimoto T, Noji T, Tanaka K. 2008. Protein kinases Fpk1p and Fpk2p are novel regulators of phospholipid asymmetry. Mol. Biol. Cell 19:1783–1797. <http://dx.doi.org/10.1091/mbc.E07-07-0646>.
 37. Takagi K, Iwamoto K, Kobayashi S, Horiuchi H, Fukuda R, Ohta A. 2012. Involvement of Golgi-associated retrograde protein complex in the recycling of the putative Dnf aminophospholipid flippases in yeast. Biochem. Biophys. Res. Commun. 417:490–494. <http://dx.doi.org/10.1016/j.bbrc.2011.11.147>.
 38. Lewis MJ, Nichols BJ, Prescianotto-Baschong C, Riezman H, Pelham HR. 2000. Specific retrieval of the exocytic SNARE Snc1p from early yeast endosomes. Mol. Biol. Cell 11:23–38. <http://dx.doi.org/10.1091/mbc.11.1.23>.
 39. Holthuis JC, Nichols BJ, Dhruvakumar S, Pelham HR. 1998. Two syntaxin homologues in the TGN/endosomal system of yeast. EMBO J. 17:113–126. <http://dx.doi.org/10.1093/emboj/17.1.113>.
 40. Siniouoglou S, Pelham HR. 2001. An effector of Ypt6p binds the SNARE Tlg1p and mediates selective fusion of vesicles with late Golgi membranes. EMBO J. 20:5991–5998. <http://dx.doi.org/10.1093/emboj/20.21.5991>.
 41. Carman GM, Han GS. 2011. Regulation of phospholipid synthesis in the yeast *Saccharomyces cerevisiae*. Annu. Rev. Biochem. 80:859–883. <http://dx.doi.org/10.1146/annurev-biochem-060409-092229>.
 42. Shindiapina P, Barlowe C. 2010. Requirements for transitional endoplasmic reticulum site structure and function in *Saccharomyces cerevisiae*. Mol. Biol. Cell 21:1530–1545. <http://dx.doi.org/10.1091/mbc.E09-07-0605>.
 43. Letts VA, Klig LS, Bae-Lee M, Carman GM, Henry SA. 1983. Isolation of the yeast structural gene for the membrane-associated enzyme phosphatidylserine synthase. Proc. Natl. Acad. Sci. U. S. A. 80:7279–7283. <http://dx.doi.org/10.1073/pnas.80.23.7279>.
 44. Gardocki ME, Jani N, Lopes JM. 2005. Phosphatidylinositol biosynthesis: biochemistry and regulation. Biochim. Biophys. Acta 1735:89–100. <http://dx.doi.org/10.1016/j.bbalip.2005.05.006>.
 45. Williams JG, McMaster CR. 1998. Scanning alanine mutagenesis of the

- CDP-alcohol phosphotransferase motif of *Saccharomyces cerevisiae* cholinephosphotransferase. *J. Biol. Chem.* 273:13482–13487. <http://dx.doi.org/10.1074/jbc.273.22.13482>.
46. Gohil VM, Thompson MN, Greenberg ML. 2005. Synthetic lethal interaction of the mitochondrial phosphatidylethanolamine and cardiolipin biosynthetic pathways in *Saccharomyces cerevisiae*. *J. Biol. Chem.* 280:35410–35416. <http://dx.doi.org/10.1074/jbc.M505478200>.
 47. Fairn GD, Hermansson M, Somerharju P, Grinstein S. 2011. Phosphatidylserine is polarized and required for proper Cdc42 localization and for development of cell polarity. *Nat. Cell Biol.* 13:1424–1430. <http://dx.doi.org/10.1038/ncb2351>.
 48. Pranke IM, Morello V, Bigay J, Gibson K, Verbavatz JM, Antonny B, Jackson CL. 2011. α -Synuclein and ALPS motifs are membrane curvature sensors whose contrasting chemistry mediates selective vesicle binding. *J. Cell Biol.* 194:89–103. <http://dx.doi.org/10.1083/jcb.201011118>.
 49. Atkinson K, Fogel S, Henry SA. 1980. Yeast mutant defective in phosphatidylserine synthesis. *J. Biol. Chem.* 255:6653–6661.
 50. Costaguta G, Duncan MC, Fernández GE, Huang GH, Payne GS. 2006. Distinct roles for TGN/endosome epsin-like adaptors Ent3p and Ent5p. *Mol. Biol. Cell* 17:3907–3920. <http://dx.doi.org/10.1091/mbc.E06-05-0410>.
 51. Trotter PJ, Pedretti J, Voelker DR. 1993. Phosphatidylserine decarboxylase from *Saccharomyces cerevisiae*. Isolation of mutants, cloning of the gene, and creation of a null allele. *J. Biol. Chem.* 268:21416–21424.
 52. Clancey CJ, Chang SC, Dowhan W. 1993. Cloning of a gene (*PSD1*) encoding phosphatidylserine decarboxylase from *Saccharomyces cerevisiae* by complementation of an *Escherichia coli* mutant. *J. Biol. Chem.* 268:24580–24590.
 53. Gulshan K, Shahi P, Moye-Rowley WS. 2010. Compartment-specific synthesis of phosphatidylethanolamine is required for normal heavy metal resistance. *Mol. Biol. Cell* 21:443–455. <http://dx.doi.org/10.1091/mbc.E09-06-0519>.
 54. Trotter PJ, Voelker DR. 1995. Identification of a non-mitochondrial phosphatidylserine decarboxylase activity (*PSD2*) in the yeast *Saccharomyces cerevisiae*. *J. Biol. Chem.* 270:6062–6070. <http://dx.doi.org/10.1074/jbc.270.11.6062>.
 55. Saba JD, Nara F, Bielawska A, Garrett S, Hannun YA. 1997. The *BST1* gene of *Saccharomyces cerevisiae* is the sphingosine-1-phosphate lyase. *J. Biol. Chem.* 272:26087–26090. <http://dx.doi.org/10.1074/jbc.272.42.26087>.
 56. Storey MK, Clay KL, Kutateladze T, Murphy RC, Overduin M, Voelker DR. 2001. Phosphatidylethanolamine has an essential role in *Saccharomyces cerevisiae* that is independent of its ability to form hexagonal phase structures. *J. Biol. Chem.* 276:48539–48548. <http://dx.doi.org/10.1074/jbc.M109043200>.
 57. Stevens HC, Malone L, Nichols JW. 2008. The putative aminophospholipid translocases, DNF1 and DNF2, are not required for 7-nitrobenz-2-oxa-1,3-diazol-4-yl-phosphatidylserine flip across the plasma membrane of *Saccharomyces cerevisiae*. *J. Biol. Chem.* 283:35060–35069. <http://dx.doi.org/10.1074/jbc.M802379200>.
 58. Baldrige RD, Graham TR. 2012. Identification of residues defining phospholipid flippase substrate specificity of type IV P-type ATPases. *Proc. Natl. Acad. Sci. U. S. A.* 109:E290–E298. <http://dx.doi.org/10.1073/pnas.1115725109>.
 59. Parsons AB, Lopez A, Givoni IE, Williams DE, Gray CA, Porter J, Chua G, Sopko R, Brost RL, Ho CH, Wang J, Ketela T, Brenner C, Brill JA, Fernandez GE, Lorenz TC, Payne GS, Ishihara S, Ohya Y, Andrews B, Hughes TR, Frey BJ, Graham TR, Andersen RJ, Boone C. 2006. Exploring the mode-of-action of bioactive compounds by chemical-genetic profiling in yeast. *Cell* 126:611–625. <http://dx.doi.org/10.1016/j.cell.2006.06.040>.
 60. Sun Y, Drubin DG. 2012. The functions of anionic phospholipids during clathrin-mediated endocytosis site initiation and vesicle formation. *J. Cell Sci.* 125:6157–6165. <http://dx.doi.org/10.1242/jcs.115741>.
 61. Kishimoto T, Yamamoto T, Tanaka K. 2005. Defects in structural integrity of ergosterol and the Cdc50p-Drs2p putative phospholipid translocase cause accumulation of endocytic membranes, onto which actin patches are assembled in yeast. *Mol. Biol. Cell* 16:5592–5609. <http://dx.doi.org/10.1091/mbc.E05-05-0452>.
 62. Uchida Y, Hasegawa J, Chinnapen D, Inoue T, Okazaki S, Kato R, Wakatsuki S, Misaki R, Koike M, Uchiyama Y, Iemura S, Natsume T, Kuwahara R, Nakagawa T, Nishikawa K, Mukai K, Miyoshi E, Taniguchi N, Sheff D, Lencer WI, Taguchi T, Arai H. 2011. Intracellular phosphatidylserine is essential for retrograde membrane traffic through endosomes. *Proc. Natl. Acad. Sci. U. S. A.* 108:15846–15851. <http://dx.doi.org/10.1073/pnas.1109101108>.
 63. Antonny B. 2011. Mechanisms of membrane curvature sensing. *Annu. Rev. Biochem.* 80:101–123. <http://dx.doi.org/10.1146/annurev-biochem-052809-155121>.
 64. Zendeheboodi Z, Yamamoto T, Sakane H, Tanaka K. 2013. Identification of a second amphipathic lipid-packing sensor-like motif that contributes to Gcs1p function in the early endosome-to-TGN pathway. *J. Biochem.* 153:573–587. <http://dx.doi.org/10.1093/jb/mvt025>.
 65. Xu P, Baldrige RD, Chi RJ, Burd CG, Graham TR. 2013. Phosphatidylserine flipping enhances membrane curvature and negative charge required for vesicular transport. *J. Cell Biol.* 202:875–886. <http://dx.doi.org/10.1083/jcb.201305094>.
 66. Verhulst PM, van der Velden LM, Oorschot V, van Faassen EE, Klumperman J, Houwen RH, Pomorski TG, Holthuis JC, Klomp LW. 2010. A flippase-independent function of ATP8B1, the protein affected in familial intrahepatic cholestasis type 1, is required for apical protein expression and microvillus formation in polarized epithelial cells. *Hepatology* 51:2049–2060. <http://dx.doi.org/10.1002/hep.23586>.
 67. Noji T, Yamamoto T, Saito K, Fujimura-Kamada K, Kondo S, Tanaka K. 2006. Mutational analysis of the Lem3p-Dnf1p putative phospholipid-translocating P-type ATPase reveals novel regulatory roles for Lem3p and a carboxyl-terminal region of Dnf1p independent of the phospholipid-translocating activity of Dnf1p in yeast. *Biochem. Biophys. Res. Commun.* 344:323–331. <http://dx.doi.org/10.1016/j.bbrc.2006.03.095>.
 68. Sikorski RS, Hieter P. 1989. A system of shuttle vectors and yeast host strains designed for efficient manipulation of DNA in *Saccharomyces cerevisiae*. *Genetics* 122:19–27.
 69. Gietz RD, Sugino A. 1988. New yeast-*Escherichia coli* shuttle vectors constructed with *in vitro* mutagenized yeast genes lacking six-base pair restriction sites. *Gene* 74:527–534. [http://dx.doi.org/10.1016/0378-1119\(88\)90185-0](http://dx.doi.org/10.1016/0378-1119(88)90185-0).